# The relationship between q profiles, transport, and sawteeth in tokamaks

F. A. Haas and A. Thyagaraja

Citation: Phys. Fluids B 3, 3388 (1991); doi: 10.1063/1.859770
View online: http://dx.doi.org/10.1063/1.859770
View Table of Contents: http://pop.aip.org/resource/1/PFBPEI/v3/i12
Published by the American Institute of Physics.

# The relationship between $q$ profiles, transport, and sawteeth in tokamaks

F. A. Haas and A. Thyagaraja
*AEA/Euratom Fusion Association, Culham Laboratory, Abingdon, OX14 3DB, United Kingdom*

(Received 23 October 1990; accepted 17 July 1991)

The purpose of this paper is to investigate the possible relationships between transport properties such as thermal diffusivity and resistivity on the one hand, and the magnetic properties such as $q$ profile and toroidal flux change on the other, in tokamaks that exist under macroscopically quasistationary conditions. It is experimentally well established that when the sources are held constant over times long compared with energy and particle confinement times, tokamak discharges can exist in a quasistationary state with or without periodic sawteeth superposed on the basic equilibrium. The principal aim of this study is to provide qualitative physical insight into the nature of such states. For simplicity, single-fluid equations are assumed and the analysis is restricted to a cylinder model. The complete set of conservation equations comprising continuity, pressure balance, Ohm's law, and energy balance are used along with appropriate sources. The conductive energy loss is assumed to occur due to an anomalous thermal diffusivity. Following earlier time-dependent studies of tokamak transport phenomenology due to the authors [Haas and Thyagaraja, Plasma Phys. Controlled Fusion **28**, 1093 (1986)], the friction force in the generalized Ohm's law is assumed to be described by an effective resistivity tensor with its principal axes in the poloidal and toroidal directions. The toroidal resistivity is taken to be of order Spitzer while the poloidal component $\eta_\theta$ is assumed to be anomalously large compared with $\eta_z$. A range of phenomena involving Ohmic discharges, auxiliary heated discharges, and noninductively driven currents is investigated. Attention is drawn to the joint implications of the conservation laws and the general forms of the constitutive relations for the structure of the profiles and conditions for the existence of equilibria. In particular, it is shown that $\beta_p > 1$ is achievable in macroscopically steady conditions, only if a sufficiently strong particle source is present *in addition* to an energy source. It also follows from the analysis that low $\beta_p$ discharges require an anomalous thermal force type term in Ohm's law, in addition to the anomalous poloidal resistivity. Recent experimental results on sawtoothing discharges are used to extend the theoretical considerations from strictly steady discharges to those involving sawteeth. A simple nonlinear dynamical model of sawtoothing is constructed and used to illustrate some of the features of sawtooth oscillations. The paper is intended to complement fuller numerical studies. It may help in understanding transport and large-scale relaxation processes like the sawtooth in tokamaks by providing a set of theoretical relations that can be subjected to a direct experimental test. It is a feature of the results that they are independent of the details of the turbulent dynamics, which are ultimately thought to be responsible both for the form and scaling of the constitutive properties considered.

## I. INTRODUCTION

Tokamaks exist in macroscopically stationary states provided external sources such as heating power, gas puffing, and loop volts are kept reasonably constant for times long compared with the confinement time. There are usually two types of time-dependent oscillations in such states. First, there is the usual microturbulence that affects all transport properties, especially the electron and ion thermal diffusivities, momentum diffusivity, and particle transport coefficients. Second, there is the large-scale time-periodic behavior found in many sawtoothing discharges, and Mirnov activity associated with $m \geqslant 2$ tearing modes in certain conditions. The subject of the present paper is an analytic consideration of macroscopically stationary discharges. We are not concerned in this work directly with the microturbulence, except insofar as to assume that it is ultimately responsible for the experimentally observed diffusion rates of energy, momentum, particles, and field. We shall also not be concerned with high $m$ tearing mode activity [for example, edge localized modes (elm's)], which is sometimes found to occur in the edge regions. We shall, however, be interested in both sawtooth-free discharges [for example, monsters in the joint European torus[1] (JET) or where sawteeth have been stabilized] and in sawtoothing discharges.[1-7] In the case of the latter, we shall rely on experiment and earlier numerical simulations[8-13] to motivate the theoretical assumptions. We should state at the outset that an analytic approach like the present one is aimed at providing theoretical insight into the possible relationships prevailing between constitutive properties of the plasma on the one hand and the profile proper-

 0899-8221/91/123388-18$02.00  

ties of density, temperature, and field, as measured by the experimentalists, on the other hand. Clearly such an approach is complementary to more detailed simulations using empirically determined constitutive relations and experimentally relevant sources and boundary conditions.

The primary interests of this paper are twofold. The first is to determine the possible relationships prevailing between macroscopic transport properties and the magnetic field structure, as defined by the $q$ profile. The second is to derive under macroscopically steady conditions (that is, when the sources of particles, momentum, energy, and current are held fixed for times long compared to the confinement time and the sawtooth repetition period) a series of relationships involving the turbulent constitutive properties such as thermal diffusivity and resistivity, and the global and local plasma parameters such as $\beta_p$. In particular, we have shown that $\beta_p > 1$ is achievable in macroscopically steady conditions, only if a sufficiently strong particle source is present *in addition* to an energy source. It also follows from our analysis that low $\beta_p$ discharges require an anomalous thermal force type term in Ohm's law in addition to the anomalous poloidal resistivity. These relations follow from the forms of the conservation laws and enable us to make a number of quantitative and qualitative statements about reactor-relevant steady conditions and possible scalings with power and current. However, we have attempted, wherever possible, to validate our phenomenologically motivated constitutive assumptions by comparison with existing tokamak experiments. We remark that an analysis in a very similar spirit to ours has been carried out by Kim and Greene.[14] However, these workers consider neoclassical forms and values for the constitutive properties. Furthermore, they exclude energy transport, thus concentrating mainly on particle transport.

We start with a brief review of the present experimental status of $q$-profile measurements. There is now a large body of experimental observations in JET and other tokamaks relating to the $q$ profile under a wide variety of conditions.[1-7] These involve several distinct direct and indirect techniques for measuring the $q$ profile—in particular, the value of $q_0$ at the magnetic axis as a function of time—and the location of the $q = 1$ radius. First, some of these results appear to show that $q_0$ can be significantly below unity, both in sawtooth-free (i.e., monsters) and sawtoothing discharges, with and without auxiliary heating. Furthermore, the observations appear to show (especially in sawtoothing discharges[2]) that $q_0$ does not vary significantly, during the ramp phase before and after a sawtooth crash. Indeed, for some techniques of determining $q_0$, the time variation of this quantity during the entire sawtooth cycle is comparable to the experimental error bars associated with the measurement. Most of the methods agree that the $q = 1$ radius changes in time up to about 30% of minor radius in JET during the ramp phase. At the crash there may be a sizable displacement, but "snakes" and other phenomena have shown that immediately after the crash the $q$ profile is not much different from the one before the crash. It must be stated that the profile measurements in the main do not have sufficient resolution in time to be instantaneous measures of $q$ during a complete sawtooth period. In TEXT,[6] for example, both a time average over many periods and a shot-to-shot averaging has been used to obtain a mean $q$ profile [i.e., a time-averaged component of $q(r,t)$]. However, measurements in JET[1,2] for example, have used instantaneous polarimetry to obtain $q_0$ as a function of time in a single pulse over three seconds encompassing many sawtooth periods. This appears to suggest that $q_0$ has a nearly steady value of about 0.7. These observations and others[5] seem to imply that the time-dependent part of the $q$ profile in sawtoothing discharges is less than or of the order of 10% of the time-averaged mean. Turning to sawtooth-free discharges in JET, the measured values of $q_0$ appear to evolve in time on the resistive time scale (of order 1 sec), steadily falling throughout the "monster" phase (of order 3 sec), reaching a minimum value just before the crash. The time-averaged value is about 0.75. It is also clear that the $q = 1$ radius in this case is increasing slowly to nearly 50% of the minor radius.

Next we review a number of recent numerical simulations of the single-fluid resistive equations, including energy transport, and designed to model sawtooth oscillations.[8-13] These simulations fall into two classes. In the first, the complete set of resistive fluid equations (sometimes simplified to the reduced equations in the tokamak ordering) are solved with certain assumptions relating to the constitutive properties such as resistivity, viscosity, and thermal diffusivity tensors. In the second class, of which Goedheer and Westerhof[13] are a good example, the complete equations are not solved but certain assumptions relating to the $m = 1$ instability of the basic time-evolving equilibrium are made in order to obtain a periodic solution. Turning to the first class, under appropriate conditions, these simulations have successfully reproduced aspects of the Kadomtsev reconnection model. In particular, adopting suitable forms (and magnitudes) for the resistivity and the thermal diffusivity, Denton *et al.*[8] have demonstrated the importance of cross-field thermal conduction in determining the properties of sawteeth oscillations. They obtain normal sawteeth, however, when skin currents form, which drive $q$ below unity at a finite radius away from the magnetic axis, with $q_0 \geqslant 1$. In contrast, the measurements of O'Rourke *et al.*[1,2] and others show that throughout all phases of the sawtooth $q_0$ remains significantly below unity, and its oscillations in time are within a few percent of its mean value.

In addition, as pointed out by Goedheer and Westerhof,[13] the sawtooth repetition period is considerably smaller than the resistive diffusion time-scale, as also indicated by experiment.[1] However, with the enhanced values of $\eta$ used in the codes,[8,12] the resistive diffusion time scale appropriate to these values is effectively of the order of the sawtooth period obtained in the simulations. It then follows, that if the simulations were to be carried out for realistic values of resistivity, a relatively fast sawtooth period could not be obtained.

Although these complete simulations model anomalous energy transport in a semiempirical manner, with prescribed forms for the thermal diffusivity tensor, they are inadequate with regard to modeling the particle transport. Thus, for complete sawtooth modeling it may be necessary to retain compressibility in the equation of continuity and use an

anomalous resistivity tensor in order to model the correct particle transport properties. That such a tensor could model the equilibrium, in the same sense that an anomalous perpendicular thermal diffusivity is needed, was pointed out by Bickerton,[15] and more recently by us.[16] During the crash when the inertial terms become important, it is necessary to retain compressibility, since $\mathbf{v}$ is not divergence-free, in general, and certainly the fluid sound speed is not large compared to the Alfvén velocity. An important general conclusion to be drawn from these numerical simulations is the influence that $\chi_\perp$ has on the results. Thus the magnitude of $\chi_\perp$, its radial variation, and its possible dependence on temperature, all appear to play a fundamental role in the simulations cited. Thus the fact whether $\chi_\perp$ is constant in space or increasing with radius bears on the nature of the calculated $q$ profiles. Aydemir *et al.*[12] noted that if $\chi_\perp$ varied with temperature in a certain fashion (differently to resistivity), the time periodicity of the solution was destroyed. They also noted certain invariance properties if $\chi_\perp$ and $\eta$ were scaled similarly in magnitude.

Turning to the work of Goedheer and Westerhof, they construct a sawtooth model using a set of one-dimensional (1-D) transport equations (ICARUS code),[13] but excluding pressure balance and poloidal Ohm's law. Assuming a constant $\chi_\perp$ within the $q = 1$ surface, they have simulated the ramp phase of the sawtooth. They consider both the Kadomtsev reconnection model and the turbulent model of Dubois and Samain.[17] The sawtooth repetition period and the crash itself are obtained using different phenomenological prescriptions in the two models. In the reconnection model the $q$ is essentially flat within the resonant radius, and does not vary much during the ramp or the crash. However, the temperature and density profiles are drastically altered everywhere within the $q = 1$ surface. In the turbulence model, the $q$ profile is approximately unchanged everywhere. The changes to the density and temperature are largely localized to the $q = 1$ radius. The authors remark that the turbulence model is in better agreement with experiment, and indeed the agreement is improved if $\chi_\perp$ is assumed to be monotonically increasing inside the $q = 1$ surface, as suggested by experimental measurements. An important conclusion that emerges from this interesting study is that the turbulence model implies a nearly time-invariant $q$ profile, right through the sawtooth process, which is not globally modified significantly by the crash. Furthermore, the incremental transport coefficients due to the crash are largely localized to the $q = 1$ radius, in total contrast to the reconnection model.

We next review briefly the raison d'être for the present investigation. Here, we are less concerned with detailed numerical simulations, and more with discovering relationships that hold by virtue of the conservation equations between transport properties like $\chi$ and $\eta$, and the $q$ profile, which the previously reviewed works emphasize. There are two parts to our study of these relationships. We first look at the complete set of transport equations in a steady or time-averaged framework in order to determine the necessary conditions for the existence of symmetric equilibrium states. In the second part we discuss more briefly in a qualitative fashion the effects of periodic sawtoothing behavior or a long-time resistive evolution superimposed on the symmetric equilibria. The analytic theory presented is intended to offer physical insight and is clearly complementary to a fuller numerical investigation of the complete set of evolution equations. We note that earlier workers have not always included the complete set of equations.

The material is organized as follows: in Sec. II the principal formulas and the results derived are highlighted for the convenience of the reader who is more interested in the predictions of the model than in the mathematical details of the derivations. Section III includes a relatively complete discussion of the hypotheses that underlie the model and results pertaining to strictly steady states. In Sec. IV, we make use of recent experimental data on sawtoothing discharges to derive time-averaged equations in the presence of sawteeth but macroscopically stationary sources. A simple model of nonlinear sawtooth dynamics is presented and used to relate observed sawtoothing parameters to theory. In Sec. V we present the conclusions in brief.

## II. AN OVERVIEW OF THE PRINCIPAL RESULTS

The purpose of this section is to pick out the principal results of this paper in a form that brings out their physical content and significance. The detailed arguments and an account of the underlying hypotheses are given in the body of the paper. For the experimentalist who is primarily interested in the possible experimentally testable relationships between magnetic plasma properties such as $q$ and $\beta$ on the one hand and transport properties such as $\chi$, $\eta$, and the profiles on the other hand, the following summary may be useful.

It is convenient to divide the results into several distinct cases. First, we consider Ohmic steady states in the absence of particle sources. In contrast to previous approaches, we explicitly link pressure balance and poloidal Ohm's law via our anomalous poloidal resistivity hypothesis.[16] The significance of this link will be discussed later in this section. It turns out that the magnetic properties such as $q$, which are conventionally related to temperature and density via the specified form of toroidal resistivity, may also be related to $\chi$. Thus, the conservation equations imply that in *steady state*, a definite numerical relation must exist between the thermal diffusivity (measured by $\chi$) and the field diffusivity (measured by $c^2\eta_z/4\pi$). We should stress that this particular relation had already been derived by us in a slightly different form earlier.[16] Thus, if the radial (conductive) heat flux is written as $Q_{\text{tot}}(r) \equiv -\chi(dp/dr)$ (this definition is appropriate in a single temperature model, as discussed in the next section), the conservation laws imply a steady solution if $\chi = c^2\eta_z/4\pi$. It is important to note that this is not an identity but an equilibrium condition that is valid, provided particle sources and radiative losses are negligible. As shown in our earlier paper,[16] this relation is readily checked in order of magnitude. This equation may be used in experimental situations in more than one way. Thus if $\chi$ is measured by one of several methods currently in use, the relation helps us to deduce (provided the assumed conditions prevail) the local value of $\eta_z$. Conversely, if the functional form of $\eta_z$ is taken as known (e.g., as in Spitzer theory) in terms of $Z_{\text{eff}}$, density, and temperature profiles, the relation and the mea-

sured values of $\chi$ enables us to deduce the $Z_{\text{eff}}$ profile (say) in terms of the others and compare directly with the *measured* $Z_{\text{eff}}$ profile. Since $\eta_z$ is obviously related to the $q$ profile through Ohm's law, the stated relation can be used to deduce the plasma thermal profile properties from the measured $q$ profile, and vice versa.

Specifically, we find that $q(r^2/a^2)$ can be written in terms of the $\chi$ profile as follows:

$$\frac{1}{q} = \frac{cV_l}{4\pi B_z}\frac{1}{x}\int_0^x \frac{dx'}{\chi(x')}, \tag{1}$$

where $V_l$ is the loop voltage and $x \equiv r^2/a^2$. It can also be shown that $q_0$, the value of $q$ at the magnetic axis, is related to $q_a$ and the profile of $\chi$ (or, equivalently, of $\eta_z$) through,

$$q_0 = q_a \chi_0 \int_0^1 \frac{dx'}{\chi(x')}, \tag{2}$$

where $\chi_0$ is the value of $\chi$ at $r = 0$. Thus it is clear that the issue of whether $q_0$ is less than unity and whether the profile of $q$ in steady state has certain monotonicity properties is shown to be related to the profile properties of $\chi$. Although it was well known that the profiles of temperature and density (through $\eta_z$) determine, in principle, the properties of $q$, the relations derived here from pressure balance and the energy equation demonstrate a more subtle connection with $\chi$.

The next group of results to be reviewed applies to the presence of auxiliary heating (or a sinklike radiative loss), in addition to Ohmic heating, but still with negligible particle sources. It turns out that the analysis is very similar to the purely Ohmic case, and indeed, the relation between $q$ and $\chi$ is not fundamentally different in the presence of auxiliary heating. However, there is a new threshold condition that must be satisfied by the current, $\chi$ and the net heating power for ensuring the existence of a steady solution. Furthermore, the relation between $\chi$ and $\eta_z$ may be shown to take the form

$$\chi = \frac{c^2\eta_z}{4\pi}\left(1 + \frac{8\pi^2 R^2 q(r)}{r^2 B_z c V_l}\int_0^r rP_0(r)dr\right). \tag{3}$$

This equation may also be written in an equivalent form upon making use of the relation

$$I_p = \pi a^2 E_z \int_0^1 \frac{dx}{\eta_z(x)}, \tag{4}$$

$$\chi = \frac{c^2\eta_z}{4\pi}\left(1 + \frac{4\pi^2 a^2 R q(r)}{r^2 B_z c I_p}\int_0^1 \frac{dx}{\eta_z}\int_0^r rP_0(r)dr\right). \tag{5}$$

The second form clearly shows that for fixed current, $Z_{\text{eff}}$, and temperature (assuming $\eta_z$ to be Spitzer, for example), as the power is increased, $\chi$ must degrade and rise above the Ohmic value to maintain equilibrium, roughly like $P/I_p^2$ at constant $B_z$.

In order to discuss the effect of particle sources, it is necessary to take into account the earlier findings of Coppi and Sharkey,[18] Bickerton,[15] and ourselves.[16] Specifically, one can introduce an effective resistivity tensor with the poloidal and toroidal directions as its principal axes. It was previously shown[16,19,20] that a wide range of tokamak transport phenomena could be represented by taking the toroidal resistivity of order $\eta_{\text{Spitzer}}$ and the poloidal resistivity to be anomalous and of order $(B_{\text{tor}}^2/B_{\text{pol}}^2)\eta_{\text{tor}}$. With these assumptions and a typical steady particle source $S_0(r)$, we show in Sec. III D, that the effect of the particle source is principally to make $B_z(r)$ nonuniform. Thus, we derive the formula,

$$\frac{B_z^2}{2}(r) = \frac{B_z^2}{2}(a) - \int_r^a \frac{4\pi v_r(r')}{c^2\eta_z(r')}\frac{B_\theta^2(r')}{h(r')}dr'. \tag{6}$$

The radial velocity $v_r(r)$ is related to the source and the plasma density via the integrated (steady) continuity equation

$$v_r(r) = \frac{1}{n(r)r}\int_0^r r'S_0(r')dr'. \tag{7}$$

The function $h(r)$ appearing in Eq. (6) is $O(1)$ and nondimensional and serves to express the assumed anomalous poloidal resistivity $\eta_\theta$:

$$\eta_\theta(r) = \eta_z h(r)(B_z^2/B_\theta^2). \tag{8}$$

We observe that the relationship between the effective transport coefficient $\eta_\theta$ and the steady-state radial particle flux $\Gamma_r = \langle c\tilde{n}\tilde{E}_\theta/B_z\rangle$ is given by

$$\Gamma_r \equiv -cn\eta_\theta j_\theta/B_z. \tag{9}$$

It should be stressed that the phenomenological proposal to represent the total friction force in terms of an effective resistivity tensor is based on simplicity. In analogy with neoclassical theory one could, in principle, envisage a more general constitutive law applicable in the presence of turbulence involving other terms, such as the addition of a thermal force in Eq. (9), for example. Such generalizations would, of course, require more transport coefficients to be determined from experiment than merely $\chi$ and $\eta_z$, $\eta_\theta$ as in the present framework. Relation (9) predicts, for example, that if there is no particle flux (i.e., $\Gamma_r = 0$), the poloidal current $j_\theta$ must vanish. This prediction can be used, in principle, to put bounds on the magnitude of turbulent thermal force terms (if any) in Ohm's law by an experimental determination of the poloidal current density at a radius where the particle flux is known to be negligible. Indeed, we consider certain low $\beta_p$ discharges in Sec. III F and show that a thermal force type term is required in addition to the anomalous poloidal resistivity to interpret such discharges. We show that these additional anomalous transport properties can reduce the achievable $\beta_p$ values in particle-source free steady states of reactor relevance to less than unity in contrast to the result when they are absent. We have also derived general relations relating $\chi$, the particle diffusivity $D$, the inward pinch velocity $V$, the resistivities $\eta_\theta$, $\eta_z$, and the anomalous thermal force coefficient $\alpha\chi$. Both the qualitative and the quantitative predictions of this phenomenological framework can be tested, in principle, by experiment.

The results of this section show that the diamagnetism of the plasma is closely related to the relative rates of particle transport (measured by $v_r$) and field transport (measured by $c^2\eta_z$). The relative change in the toroidal flux, $\Delta\Psi_{\text{tor}}/\Psi_{\text{tor}}$ is $O\left[(a^2/q_a^2R^2)\{\Gamma_r a/c^2 n\eta_z\}\right]$. Finally, we consider qualitatively the effect of noninductive current drive. It is then shown that

$$\frac{4\pi\chi}{c^2\eta_z} = 1 - \frac{4\pi}{crB_\theta}\int_0^r j_z^N r\,dr + \frac{4\pi}{E_z crB_\theta}\int_0^r P_0(r) r\,dr$$

$$= 1 - \frac{4\pi}{crB_\theta}\int_0^r j_z^N r\,dr + \left(\frac{8\pi^2 R^2 q(r)}{cr^2 B_z V_l}\right)\int_0^r P_0(r) r\,dr. \tag{10}$$

In Eq. (10), the loop volts $V_l$ are related to the current and $\eta_z$ by

$$V_l = \frac{R(I^{\rm tot} - I^N)}{\int_0^a (r\,dr/\eta_z)}, \tag{11}$$

and $j_z^N$ is the current density attributed to the noninductive current source. We apply this result to a situation when an increase in the noninductively driven current at constant temperature and total current is experimentally realized. It can be deduced from the equations that in such a case, the loop voltage and the plasma density must decrease. We have also discussed the effect of the current drive efficiency $I^N/P^N$ (where $P^N$ is the auxiliary heating power absorbed by the plasma due to the current drive source) on the degradation or otherwise of $\chi$ at constant temperature.

In Sec. IV we have made use of available experimental results about sawtoothing discharges, in order to derive sawtooth-averaged transport equations. These equations are then shown to be interpretable in terms of the steady-state theory discussed in Sec. III. Although it is not yet possible, in the absence of a fundamental understanding of the constitutive properties $\chi$ and $\eta$ appropriate to actual experiments, to give a proper dynamical theory of the sawtooth oscillations observed in tokamaks, we have constructed a very simple set of nonlinear equations, which appear to be capable of reproducing the essential features of sawteeth. The parameters of this model can be directly related to experimentally measurable quantities. Using this model and our earlier[21] analysis of the nonlinearly saturated $m = 1$ tearing mode, a very crude estimate of the ratio of the crash time scale to the sawtooth period can be obtained. Thus we have

$$\tau_{\rm crash}/\tau_{\rm ramp} = O\,[r_i^2 q'(r_i)^2]. \tag{12}$$

Using the relevant JET data,[3,4] and setting $\tau_{\rm ramp} = 300$ msec, $dq(r_i)/dr = 0.04\ {\rm m}^{-1}$, and $r_i = 0.4$ m, then $\tau_{\rm crash}$ is $O(75\,\mu{\rm sec})$ from Eq. (2), is not inconsistent with the experimentally estimated value of $O(100\ \mu{\rm sec})$. This concludes our overview of the results.

## III. PROPERTIES OF THE CYLINDRICAL STEADY STATE

We begin by considering the simple single-fluid cylindrical model of the complete set of tokamak transport equations. The general forms of these are exactly those of the Braginskii equations with $T_e = T_i$. However, it must be understood in the following discussion that the constitutive properties need not be (and, in general, will not be) classical or neoclassical in form or numerical value. The discussion assumes that these properties (including their possible dependences on the plasma variables) are known, as also the particle, momentum, energy, and current sources. The theory is largely confined to an account of the plasma interior (i.e., sawtooth and confinement zones). The edge physics will not be considered explicitly, but represented by appropriate boundary conditions. Since the purpose of the model is to attain insight and not detailed numerical agreement with experiment, which is in any event conditional on the accuracy with which the constitutive relations are known, attention is restricted to cylindrical geometry. We start with equations where the derivatives satisfy $\partial/\partial t = \partial/\partial\theta = \partial/\partial z \equiv 0$. Thus we initially explore the properties of a true steady solution. The governing equations and the boundary conditions together determine the radial variations of the plasma variables, $n(r)$, $T(r)$, $p(r)$, $v_r(r)$, $B_z(r)$, and $B_\theta(r)$.

### A. Particle-source free equilibrium theory

We first consider the problem of determining the steady state in cylindrical tokamak geometry with no particle sources. We assume that the auxiliary heating power density $P_0(r)$ is specified. It will be obvious from the analysis that $P_0(r)$ can depend on plasma properties, such as $n$ and $T$, without altering our results in any way (other than complicating the formal expressions). The thermal diffusivity $\chi$ and resistivity tensor are assumed to be arbitrary functions of $n$, $T$, $B$, and $r$. We follow our earlier proposal[16] and assume that the principal directions of the effective (anomalous) resistivity tensor are "toroidal" (i.e., along the $z$ axis in the present discussion) and "poloidal" (i.e., in the $\theta$ direction). The values and/or functional forms of $\eta_z$ and $\eta_\theta$ will be discussed in detail later. For the present they may be formally assumed to be positive functions of the plasma variables and $r$. Some physical arguments in support of our hypothesis are given in Sec. III G.

From the steady-state continuity equation it follows that $v_r(r) \equiv 0$. From the poloidal Ohm's law we derive the result $j_\theta(r) \equiv 0$. This shows that $B_z$ is uniform in steady state in the absence of particle sources. The remaining single-fluid equations are

$$\frac{dp}{dr} = \frac{-j_z B_\theta}{c}, \tag{13}$$

$$j_z = \frac{c}{4\pi}\frac{1}{r}\frac{d(rB_\theta)}{dr}, \tag{14}$$

$$E_z = \eta_z j_z, \tag{15}$$

where $E_z$ is a constant to be determined from the boundary condition that the total plasma current is specified, or equivalently, $q_a$. Alternatively, we can regard $E_z$ (or the loop volts $V_l = 2\pi R E_z$) as a specified constant.

In the absence of convection due to particle sources, the total radial heat flux $Q_{\rm tot}(r)$ is conventionally parametrized in a two-temperature model in the form $Q_{\rm tot}(r) \equiv -n[\chi_i(dT_i/dr) + \chi_e(dT_e/dr)]$, where $\chi_i$, $\chi_e$ are the experimentally estimated thermal diffusivities. It should be stressed that this particular form of the conductive heat flux is suggested by analogy with Braginskii and neoclassical expressions. As far as turbulent transport is concerned, in a single-temperature model, earlier theoretical workers have found the parametrization $Q_{\rm tot}(r) \equiv -\chi_{\rm eff}(dp/dr)$ convenient (see, for example, Aydemir *et al.*[12] and Hamaguchi and Horton[22]). Of course, it follows that $\chi_{\rm eff}$ thus defined is

related to $\chi_i$, $\chi_e$ through, $\chi_{\text{eff}} \equiv n[\chi_i(dT_i/dp) + \chi_e(dT_e/dp)]$. Thus experimental knowledge of $\chi_i$, $\chi_e$ and the temperature and density profiles is entirely equivalent to a knowledge of $\chi_{\text{eff}}$, which can also be expressed as a weighted average of the individual diffusivities involving $T_i/T_e$ and the well-known expressions for $\eta_i \equiv d \log T_i / d \log n$ and $\eta_e$. It turns out for the purposes of the present paper to be convenient to use $\chi_{\text{eff}}$ as defined. We drop the suffix "effective" in the rest of the analysis. The steady-state energy equation then takes the form

$$\frac{1}{r}\frac{d}{dr}\left(r\chi\frac{dp}{dr}\right) + E_z j_z + P_0(r) = 0. \tag{16}$$

We now show that Eqs. (13), (14), and (16) effectively determine the current profile independently of $\eta_z$. Once $j_z$ is obtained, Eqs. (13) and (15) determine the density and temperature profiles. Substituting for $dp/dr$ from Eq. (13) in (16), we obtain

$$-\frac{1}{4\pi}\frac{1}{r}\frac{d}{dr}\left(r\chi B_\theta \frac{1}{r}\frac{d}{dr}(rB_\theta)\right) + \frac{cE_z}{4\pi}\frac{1}{r}\frac{d}{dr}(rB_\theta) + P_0(r) = 0. \tag{17}$$

Integrating, we obtain

$$-r\chi\frac{B_\theta}{r}\frac{d}{dr}(rB_\theta) + cE_z rB_\theta + 4\pi\int_0^r rP_0(r)dr = 0. \tag{18}$$

We now transform Eq. (18) to a nondimensional form. To this end we write $B_\theta = rB_z/Rq(r)$ and take $x = r^2/a^2$. Thus we obtain

$$\chi\frac{d}{dx}\left(\frac{x}{q}\right) = \frac{cE_z R}{2B_z} + \frac{\pi R^2}{B_z^2}\frac{\int_0^x P_0(x')dx'}{x/q}. \tag{19}$$

We now write $\chi \equiv \chi_0 \kappa(x)$, where $\kappa(x)$ is a profile function such that $\kappa(0) = 1$. We introduce the definitions $P_0 \equiv Pf(x)$ with $f(0) = 1$, and

$$\lambda \equiv cE_z R/2B_z\chi_0, \quad \mu \equiv \pi R^2 P/B_z^2\chi_0 \tag{20}$$

$$\mu\Pi(x) \equiv \frac{\pi R^2 P}{B_z^2\chi_0}\int_0^x f(x')dx'. \tag{21}$$

We note that $P, f(x)$ can be positive or negative depending on whether there is net heating or cooling. However, $\chi_0$ and $\kappa(x)$ must always be positive. Equation (19) may now be rewritten in the compact form

$$\kappa(x)\frac{d}{dx}\left(\frac{x}{q}\right) = \lambda + \mu\frac{\Pi(x)}{x/q}. \tag{22}$$

We now introduce the function

$$\xi(x) = \frac{\int_0^x [dx'/\kappa(x')]}{\int_0^1 [dx'/\kappa(x')]}. \tag{23}$$

It is useful in what follows to define the harmonic mean $\bar{\kappa}$ of the profile function $\kappa(x)$ with the equation

$$\bar{\kappa} = \left(\int_0^1 \frac{dx'}{\kappa(x')}\right)^{-1}. \tag{24}$$

Note that with these definitions the equivalent radial variable $\xi(x)$ is monotonic with $x$, with the property $\xi(0) = 0$ and $\xi(1) = 1$. The variable $x$ can always be obtained as a function of $\xi$ by inverting Eq. (23). Introducing the new dependent variable $\Theta(\xi) \equiv x/q$, and regarding $\Pi$ as as a function of $\xi$ [i.e., as $\Pi(\xi)$], Eq. (22) obviously transforms to

$$\frac{d\Theta}{d\xi} = \frac{\lambda}{\bar{\kappa}} + \frac{\mu}{\bar{\kappa}}\frac{\Pi(\xi)}{\Theta}. \tag{25}$$

Note that since $d\Pi/d\xi = (d\Pi/dx)(dx/d\xi) = f(x)[\kappa(x)/\bar{\kappa}]$,

$$\frac{d\Pi}{d\xi}(\xi = 0) = \frac{1}{\bar{\kappa}} \tag{26}$$

Eq. (25) shows that as $\xi \to 0$ and $x \to 0$, $\Theta(\xi)$ is approximated by $\Theta'(0)\xi + O(\xi^2)$, where $\Theta'(0) = (d\Theta/dx)(dx/d\xi)|_{\xi=0} = 1/q_0\bar{\kappa}$. Evaluating Eq. (25) at the origin we then obtain the exact relation

$$1/q_0 = \lambda + \mu q_0. \tag{27}$$

We note that the value of $q_0$ is entirely independent of the profile functions $\kappa(x)$ and $f(x)$, normalized as above. It only depends on the loop volts, $B_z$, $\chi_0$, and $P$. Thus given the values of $V_l$, $B_z$, $\chi_0$, $P$, and $R$, $q_0$ is determined by (for positive $P$)

$$q_0 = (1/2\mu)[(\lambda^2 + 4\mu)^{1/2} - \lambda]. \tag{28}$$

For negative $P$, we have the relation,

$$q_0 = -(1/2\mu)[(\lambda^2 + 4\mu)^{1/2} + \lambda]. \tag{29}$$

In this case we require the inequality,

$$\lambda^2 > -4\mu. \tag{30}$$

Equation (28) shows that if $P$ is positive a physically reasonable $q_0$ always exists for any given positive loop voltage.

We now consider Eq. (25) in the physically important special case when $\mu \geqslant 0$ and $\Pi(x)$ [see Eq. (21)] is positive in the range $0 < x < 1$. This corresponds to net heating overall (auxiliary heating plus radiation greater than zero). Thus even if $f(x)$ in Eq. (21) is negative in some parts of the discharge, all we require in this case is $\int_0^x f(x')dx' \geqslant 0$ for all $x$, and $f(0) = 1$. Although we shall not present the argument here, it is a straightforward matter to continuously extend the solutions for $\mu > 0$ into the $\mu < 0$ regime; this would apply to the case of Ohmic heating and radiative loss, say.

Putting $\zeta(\xi) = \Theta^2(\xi)$, then $\zeta$ satisfies

$$\frac{d\zeta}{d\xi} = \frac{2\lambda}{\bar{\kappa}}\zeta^{1/2} + 2\frac{\mu}{\bar{\kappa}}\Pi(\xi), \tag{31}$$

which is equivalent (using the boundary condition $\Theta \to 0$ as $\zeta \to 0$) to the nonlinear integral equation

$$\zeta(\xi) = \frac{2\lambda}{\bar{\kappa}}\int_0^\xi \zeta^{1/2}(\xi')d\xi' + \frac{2\mu}{\bar{\kappa}}\int_0^\xi \Pi(\xi')d\xi'. \tag{32}$$

It is follows from Eq. (32) using standard iterative methods that Eq. (31) always has a solution $\zeta(\xi,\lambda,\mu,\bar{\kappa}:\Pi)$ with the following properties: for given positive $\lambda$ and $\bar{\kappa}$, $\zeta$ is a nonnegative, monotonic increasing function of $\xi$ with $\zeta(0) = 0$ and $\zeta^{1/2}(1) = \Theta(1) = 1/q_a$. The latter satisfies the bounds

$$\frac{\lambda}{\bar{\kappa}} + \left(\frac{\lambda^2}{\bar{\kappa}^2} + \frac{2\mu}{\bar{\kappa}}\int_0^1 \Pi(\xi)d\xi\right)^{1/2} \geqslant \frac{1}{q_a} \geqslant \frac{\lambda}{2\bar{\kappa}} + \frac{1}{2}\left(\frac{\lambda^2}{\bar{\kappa}^2} + \frac{4\mu}{\bar{\kappa}}\int_0^1 \Pi(\xi)d\xi\right)^{1/2}. \tag{33}$$

Furthermore, $1/q_a$ rises with increasing $\mu$ for fixed $\lambda$, and also with increasing $\lambda$ for fixed $\mu$. The solution is unique. The above result shows that for given loop volts, $\chi$, and power a unique solution always exists with $1/q_a$ satisfying Eq. (33), and $1/q_0$ satisfying Eq. (28).

On the other hand if $\chi$, $1/q_a$, and power are given, a unique solution with $\lambda(1/q_a,\mu,\chi)>0$ exists, if and only if the threshold condition

$$\frac{1}{q_a^2} \geqslant \frac{\mu}{\bar{\kappa}} \int_0^1 \Pi(\xi')d\xi' \tag{34}$$

holds. It is of interest to note that for Ohmic conditions a unique solution always exists, and satisfies

$$1/q_a = \lambda/\bar{\kappa}. \tag{35}$$

From Eq. (25) we now show that $q(\xi)$ is monotonically increasing, providing only that $\kappa(x)$ is monotonically increasing and $f(x)$ is monotonically decreasing or constant for $\mu \geqslant 0$ (Ohmic and/or auxiliary heating). We integrate Eq. (22) generally, and write

$$\Theta(x) \equiv \frac{x}{q} = \lambda \int_0^x \frac{dx'}{\kappa(x')} + \mu \int_0^x \frac{\Pi(x')dx'}{\kappa(x')\Theta(x')}. \tag{36}$$

This equation implies

$$\frac{1}{q} = \frac{\lambda}{x} \int_0^x \frac{dx'}{\kappa(x')} + \frac{\mu}{x} \int_0^x \frac{\Pi(x')dx'}{\kappa(x')\Theta(x')}. \tag{37}$$

We now show that both the terms on the right-hand side are actually decreasing functions of $x$, for the assumed conditions. First, since $\kappa(x)$ is increasing in $x$, the harmonic mean $(1/x)\int_0^x [dx'/\kappa(x')]$ is obviously a decreasing function of $x$. To show that the average $(1/x)\int_0^x [\Pi(x')dx'/\kappa(x')\Theta(x')]$ is decreasing with $x$ for monotonic rising $\kappa$ and decreasing $f(x)$ [see Eq. (21)] is only slightly more difficult. Thus we note that Eq. (22) or (25) indicates that $\Theta$ is monotonically increasing and does so at a rate faster than $\lambda \int_0^x [dx'/\kappa(x')]$. Turning to $\Pi(x')$, since $\Pi = \int_0^x f(x')dx'$, and $f(x')$ is assumed to decrease, it is obvious that $\Pi(x')/\Theta(x')$ increases at most like $\{(1/x')\int_0^{x'} [dx''/\kappa(x'')]\}^{-1}$. But the function $\kappa(x')(1/x')\int_0^{x'} [dx''/\kappa(x'')]$ is clearly increasing as a function of $x'$ if $\kappa$ is increasing. It is now obvious that the average is monotonically decreasing. We have therefore established that $q$ must be monotonically rising under the given very general assumptions.

### B. An exactly soluble model

We note that from a physical point of view, while the above general results are satisfactory, the scaling relations are not explicit equations, but require the numerical determination of $\Theta(\xi)$. We note below that Eq. (25), or equivalently Eq. (32), can be solved exactly in closed form for arbitrary $\lambda$, $\kappa(x)$, and $\mu$, subject to a particular assumption concerning $\Pi(\xi)$. Thus if $\Pi(\xi)$ is taken proportional to $\xi$, Eq. (25) can be solved exactly without any further assumptions. Before exhibiting the solution and discussing its properties, we consider the physical significance of this assumption. Quite generally, if $\Pi(\xi)$ can be expanded in a Taylor series about $\xi = 0$, and the first term proportional to $\xi$ dominates, the assumption is a good approximation. Alternatively, the expression for $d\Pi/d\xi$ given before Eq. (26) shows that $\Pi(\xi)$ would be linear in $\xi$, provided $f(x) = 1/\kappa(x)$ is a good approximation to $f(x)$. Since experimental $\kappa(x)$ tend to be monotonic increasing toward the edge, qualitatively, this profile for the power corresponds to auxiliary heating peaking at the center in a way related to the inverse of the $\chi$ profile. Making this assumption and using Eq. (26), Eq. (25) transforms to

$$\frac{d\Theta}{d\xi} = \frac{\lambda}{\bar{\kappa}} + \frac{\mu}{\bar{\kappa}^2} \frac{\xi}{\Theta}. \tag{38}$$

It is immediate that $\Theta = \xi/q_a$ is the only solution of Eq. (38) satisfying $\Theta(0) = 0$ and $\Theta(1) = 1/q_a$, provided $\lambda$, $\bar{\kappa}$, $\mu$, and $q_a$ (all constants) are related by the exact scaling law

$$\frac{1}{q_a} = \frac{\lambda}{\bar{\kappa}} + \frac{\mu q_a}{\bar{\kappa}^2}, \tag{39}$$

Eq. (38) may be rearranged to give

$$\lambda = (\bar{\kappa}/q_a) - (\mu q_a/\bar{\kappa}). \tag{40}$$

This equation shows that for $\mu > 0$ a physical solution exists only if the threshold condition $1/q_a^2 \geqslant \mu/\bar{\kappa}^2$ holds. In this case the loop volts or $\lambda$ always increase with $1/q_a$ as in Ohmic heating. Furthermore, for a given current, increasing the heating input decreases the loop volts up to the threshold. If $\mu = -|\mu|$ (corresponding to cooling), $\lambda$ is not monotonic with current. For small currents the loop volts are essentially determined by the radiative loss, and decreases with increasing current. For small $q_a$ (large current) $\lambda$ behaves as in Ohmic heating, and increases with current. There is an optimum current for any given radiative loss $|\mu|$, such that $\lambda$ takes the minimum value. Thus $\lambda_{\min} = 2|\mu|^{1/2}$ and $q_a = \bar{\kappa}/|\mu|^{1/2}$. Returning to Eq. (28) we find $q_0$ in terms of $q_a$, $\mu$, and $\bar{\kappa}$. Thus using Eq. (38) we derive the result (for $\mu$ or $P > 0$)

$$q_0 = q_a/\bar{\kappa}. \tag{41}$$

Note that the auxiliary heating has dropped out and relation (41) is identical with that for Ohmic heating in this model. Also note that $\bar{\kappa}$ must be larger than $q_a$ for $q_0$ to be less than unity. From the definition, Eq. (24), this is possible, for example, if $\kappa(x)$ rises from 1 at $x = 0$ monotonically to a sufficiently large value. Thus, take $q_a = 4.0$ and $\kappa(x) = \exp(4x)$, then $q_0 \simeq 0.75$. It is important to observe that $q_0$ and $q_a$ are related only through the profile of $\chi$ and not on $\chi_0$ and $P$ individually.

Provided $q_a/\bar{\kappa} < 1$, then the $q = 1$ radius is given by the equation

$$x_i = \frac{\bar{\kappa}}{q_a} \int_0^{x_i} \frac{dx'}{\kappa(x')}. \tag{42}$$

It is clear that this equation has a unique solution $x_i$, for $(0 < x_i < 1)$, if and only if $q_0$ from Eq. (39) and $q_a$ satisfy $q_0 < 1$ and $q_a > 1$. Since we have already shown that $q$ must be monotonically rising under very general conditions, the above result follows.

### C. Physical consequences of the theory

We begin with the Ohmic case, that is, no auxiliary heating or radiation losses ($\mu = 0$). As noted previously, this is

actually a special case of our exactly solved model (Sec. III B). In view of the great importance of this case, and the insight it offers, we discuss this first. We note from our exact solution that the $q$ profile in Ohmic heating can be expressed with no assumptions on the behavior of $\kappa$ (other than positivity) in the form

$$q(x) = q_a x \frac{\int_0^1 [dx'/\chi(x')]}{\int_0^x [dx'/\chi(x')]}, \tag{43}$$

where $x = r^2/a^2$. This formula shows that the $q$ profile in Ohmic heating is totally determined by $q_a$ and the distribution of $\chi$. Thus it may be used both ways experimentally to determine $q$ if $\chi$ is known, or $\chi$ if $q$ is known. If $\chi(x)$ is monotonically increasing, we have proved that $q(x)$ is also monotonically increasing. We have shown that $q_0$ can be less than unity for given $q_a$, if and only if $q_a > 1$ and

$$q_a \chi(0) \int_0^1 \frac{dx'}{\chi(x')} < 1. \tag{44}$$

If $\chi$ is monotonically increasing and Eq. (44) holds, then there is a unique inversion radius. Formula (43) also shows that Ohmic tokamaks, in the absence of particle sources and given $q_a$, will have the same $q$ profile, if and only if their $\chi$ profiles are identical. This conclusion is totally independent of the mechanisms that are responsible for the $\chi$ profile in the first place. Indeed, the $\chi$ can, in principle, be classical, neoclassical, turbulent in origin, or any combination. In other words $\chi$ only needs to be an "effective" constitutive property of the plasma.

Returning to the general equation, Eq. (18), if $P_0 \equiv 0$,

$$-\frac{\chi}{r}\frac{d}{dr}(rB_\theta) + cE_z = 0. \tag{45}$$

Substituting in Eq. (15), and using Ampère's law we obtain the general equation

$$\chi = c^2\eta_z/4\pi. \tag{46}$$

From the pressure balance equation we derive the relation

$$n(r)T(r) = n(a)T(a) - \frac{1}{c}\int_a^r j_z B_\theta \, dr'. \tag{47}$$

The physical interpretation of Eq. (46) is that in the absence of particle sources, under Ohmic steady conditions, equilibrium is possible only if the thermal diffusivity ($\chi$) is numerically equal to the field diffusivity ($c^2\eta_z/4\pi$) at every point of the discharge. This relation is based on general conservation laws and is again entirely independent of the nature of the constitutive properties $\chi$ and $\eta_z$. It cannot be stressed too strongly that Eq. (46) is an *equation* and not an identity. In fact, quite generally, Eqs. (46) and (47), together with Eq. (41) and $B_z$, $q_a$, $R$, and $a$ are two equations to determine the two unknowns $n(r)$ and $T(r)$, given $n(a)$, $T(a)$. In addition, one must, of course, specify the numerical value of $\chi(r)$ and the functional relationship between $n$, $T$, and $\eta_z$. To illustrate this process in a physically interesting case, we consider the following simple example. We assume that $\chi(r)$ has been measured in an Ohmic device with a given $q_a$. We assume $\eta_z$ is given by the Spitzer formula $\eta_z \equiv \eta_z(a)(T_a/T)^{3/2}$. Equation (46) says $T(r) = \{(c^2/4\pi)[\eta_z(a)T_a^{3/2}/\chi(r)]\}$, which also requires for consistency $\chi(a) = c^2\eta_z(a)/4\pi$. Substituting for $j_z$, $B_\theta$, from Eqs. (13) and (43) and $T(r)$ in Eq. (47), we obtain $n(r)$. Of course these relations can also be used to determine $\chi$ and $\eta_z$ if experiment gives $n$, $T$, and $q$. In general, for non-Spitzer functional dependence of $\eta_z$, the actual solutions for $n$ and $T$ are not explicit as here, but the principles remain the same.

Moving on to the auxiliary heated case, we have derived under rather general conditions the following results:

(i) For fixed $q_a$ as the heating power is increased, provided the power density profile is peaked in the center and decreasing outward, the $q$ profile is monotonically increasing. Furthermore, there is an exact relation [embodied in Eqs. (27)–(29)], which holds independently of any assumptions about the profile of $\chi$ and the power. This gives $q_0$ in terms of the loop volts, $\chi_0$, $P_0$, $B_z$, and $R$. It shows that for a fixed loop voltage, an increase of heating lowers $q_0$. Note that in the exactly solved model $q_0 = q_a/\bar{\kappa}$, and is hence independent of power for fixed current, as in the Ohmic case. In the general case $q_0$ is mainly determined by $q_a$ and depends on power relatively weakly.

(ii) There exists a general threshold relation, Eq. (33). It is remarkable that the toroidal field $B_z$ is not involved in this relation as it cancels out. Alternatively, for a given $\chi$ and power, the current must be large enough for the unique steady solution to exist. The peak temperatures and densities are determined for a given power, current, and $\chi$, by the properties of the effective $\eta_z$ and the pressure balance. In general, $p$ must scale like $I_p^2$ and hence there is a tradeoff between $n$ and $T$ for a given current. We note from Eqs. (13), (15), and (18), we obtain a generalization of Eq. (46),

$$\chi = \frac{c^2\eta_z}{4\pi}\left(1 + \frac{8\pi^2 R^2 q(r)}{r^2 B_z c V_l}\int_0^r rP_0(r)dr\right), \tag{48}$$

or equivalently, making use of the relation

$$I_p = \pi a^2 E_z \int_0^1 \frac{dx}{\eta_z(x)}, \tag{49}$$

$$\chi = \frac{c^2\eta_z}{4\pi}\left(1 + \frac{4\pi^2 a^2 R q(r)}{r^2 B_z c I_p}\int_0^1 \frac{dx}{\eta_z}\int_0^r rP_0(r)dr\right). \tag{50}$$

These equations for local $\chi(r)$ can be interpreted in two equivalent ways. If $\chi$ is given, $\eta_z$ is Spitzer, and the power is raised keeping the loop volts fixed, the temperature is increased, as might be expected. On the other hand, for a fixed current profile and $\eta_z$ (i.e., temperature), Eq. (50) clearly shows that as the power is increased $\chi$ must degrade, and rises above the Ohmic value to maintain equilibrium, roughly like $P/I_p^2$ independently of $B_z$. Conversely, for *fixed* $\chi$, the temperature scales like $P^{2/3}/I_p^{4/3}$ as power and current are independently varied. Indeed, if $\eta_z$ is taken to be Spitzer, Eq. (50) may be rewritten in a physically more appealing form. Thus, in the absence of auxiliary heating, $\chi_{\text{Ohmic}}(T) = c^2\eta_z/4\pi$, where $T$ is the appropriate temperature. If we now imagine auxiliary heating is applied at the *same total current and no particle sources*, let the temperature rise to $T_{\text{aux}}(r)$. We may obviously deduce from Eq. (50) that,

$$\chi_{\rm aux}(r)=\chi_{\rm Ohmic}(T_{\rm Ohmic})\left(\frac{T_{\rm Ohmic}}{T_{\rm aux}}\right)^{3/2}\times\left(1+\frac{4\pi^2a^2Rq(r)}{r^2B_zcI_p}\int_0^1\frac{dx}{\eta_z(T_{\rm aux})}\int_0^r rP_0(r)dr\right). \tag{51}$$

This formula shows the degradation of $\chi_{\rm aux}$ relative to $\chi_{\rm Ohmic}$ due to a power source in the *absence* of significant particle sources at constant current, taking into account the temperature variation of Spitzer resistivity. It could be directly tested in experiment, given measured values of the temperatures.

We should stress that, strictly speaking, these results only apply to the $\beta_p=1$ situation (see Secs. III D and III F for a more complete discussion). In the case where particle sources and/or thermal force terms in Ohm's law play a role, $\beta_p$ is not necessarily equal to unity. In our earlier work[16] we investigated the effects of particle sources (without thermal force terms), allowing for the fact (as suggested by experiment) that the local $\chi$ degrades through a dependence on *local* poloidal $\beta(=p/B_\theta^2)$ alone. For a quadratic dependence, $\chi\propto(p/B_\theta^2)^2$ and a fixed particle source, we found the global energy confinement time, $\tau_{\rm conf}$, to scale like $I_p^{1.7}P^{-0.6}$—a result roughly consistent with that observed to occur in a variety of tokamaks using different forms of auxiliary heating. Finally, it is important to bear in mind that these analyses apply only to steady conditions, but which are, however of reactor interest. Transients are best investigated using the full time-dependent equations considered in our previous work,[16] possibly including thermal force type terms in the turbulent form of Ohm's law.

### D. Inclusion of particle sources and convection

The preceding discussion considered a model in which there are strictly no particle sources and no convection. As shown previously, this requires a specification of $\chi$, $\eta_z$, and power. In order to discuss particle sources in a fashion consistent with tokamak experiments, it is necessary[15,16,19] to consider the poloidal friction force and the relations between the effective poloidal resistivity $\eta_\theta$ and $\eta_z$.

The argument can be put on a firm analytical footing as follows. Consider a steady particle source $S_0(r)\geqslant 0$ that[18] is monotonically rising toward $r=a$. Such a source is typical for Ohmic tokamaks with gas puff and serves to illustrate the ideas. From the continuity equation,

$$v_r(r)=\frac{1}{n(r)r}\int_0^r r'S_0(r')dr'. \tag{52}$$

Typically $v_r$ rises monotonically from $v_r=0$ at $r=0$ to a finite, positive maximum value at $r=a$. The poloidal Ohm's law in steady state can always be written in the general form

$$-[v_r(r)/c]B_z(r)=F_\theta(r)=\eta_\theta j_\theta, \tag{53}$$

where the friction force $F_\theta$ is expressed in terms of $j_\theta$ using the effective poloidal resistivity[16,19] coefficient $\eta_\theta$. In general, for the complete plasma transport equations to be determinate, at least *three* constitutive properties $\eta_z$, $\eta_\theta$, and $\chi$ have to be specified. If the resistivity is assumed nearly isotropic (in Spitzer theory the parallel and perpendicular resistivities differ by a factor of 2), $\eta_\theta\simeq\eta_z$. Without any assumptions, we have

$$j_\theta=-[v_r(r)/c\eta_\theta]B_z. \tag{54}$$

It follows therefore that

$$\frac{dB_z}{dr}=\left(\frac{4\pi v_r(r)}{c^2\eta_\theta}\right)B_z. \tag{55}$$

If the source (or equivalently $v_r$) and $\eta_\theta$ are known, this equation, together with the boundary value, $B_z(a)$, gives the "toroidal flux" change relative to the vacuum field. We also derive the generalized form of the pressure balance, Eq. (13):

$$\frac{dp}{dr}=-\left(\frac{v_r(r)}{c^2\eta_\theta}\right)B_z^2-j_z\frac{B_\theta}{c}. \tag{56}$$

Several deductions are immediately apparent from Eqs. (55) and (56). First, if $v_r$ is positive [which it is for $S_0$ positive everywhere, or, more generally, for $(1/r)\int_0^r r'S_0(r')dr'\geqslant 0$ for all $r$], $B_z(r)$ is monotonically increasing [i.e., $B_z(r)\leqslant B_z(a)$].

Second, if $c^2\eta_\theta\simeq c^2\eta_z\simeq 4\pi\chi$, the pressure balance condition requires the ordering

$$(v_ra/\chi)\leqslant B_\theta^2/B_z^2. \tag{57}$$

However, in the works cited earlier[15,16,18,19] it was demonstrated that there are many situations in tokamaks (especially near $r=a$), where convection could be comparable with conduction (anomalous). Thus, writing

$$\frac{v_r}{c^2\eta_\theta}B_z^2\equiv\left(\frac{v_r}{c^2\eta_z}\right)\left(\frac{\eta_z}{\eta_\theta}\right)B_z^2$$

and setting

$$\left(\frac{v_r}{c^2\eta_z}\right)\left(\frac{\eta_z}{\eta_\theta}\right)B_z^2\simeq\frac{j_zB_\theta}{c}\simeq\frac{B_\theta^2}{a},$$

we find that the ordering, $av_r/c^2\eta_z\simeq av_r/\chi\simeq O(1)$ is compatible with pressure balance (and hence equilibrium) if and only if $(\eta_\theta/\eta_z)\geqslant(B_z^2/B_\theta^2)$. This is also obvious from Eq. (55), which shows that the ordering $\eta_\theta\simeq\eta_z$, $v_ra/c^2\eta_z\simeq O(1)$ implies that $\Delta B_z\equiv B_z(a)-B_z(0)\simeq O[B_z(a)]$. This, of course, is simply incorrect for tokamaks.

As we had shown earlier, a number of macroscopic tokamak phenomena can be interpreted by the full set of conservation equations provided $\eta_z\simeq\eta_{\rm Spitzer}$, $\eta_\theta\simeq\eta_{\rm Spitzer}(B_z^2/B_\theta^2)$. If this constitutive ordering is assumed, the pressure balance relation becomes

$$\frac{dp}{dr}=-\left(\frac{v_r}{c^2\eta_z}\right)\left(\frac{B_\theta^2}{h(r)}\right)-\frac{B_\theta}{4\pi}\frac{1}{r}\frac{d}{dr}(rB_\theta), \tag{58}$$

where $h(r)$ is an $O(1)$, nondimensional constitutive profile function, such that

$$\eta_\theta=\eta_z[(B_z^2/B_\theta^2)]h(r). \tag{59}$$

We also have from Eq. (55),

$$\frac{dB_z^2}{dr}=\left(\frac{8\pi v_r}{c^2\eta_z}\right)\left(\frac{B_\theta^2}{h(r)}\right). \tag{60}$$

If the sources $S_0$ are such that the convection parameter $8\pi v_r a/c^2\eta_z \sim v_r a/\chi \ll 1$, the pressure balance Eq. (13) is an excellent approximation. If $8\pi v_r(a)[a/c^2\eta_z(a)] \simeq O(1)$, which could be the case at the edge, the theory presented earlier must be modified and involves an extra loss term in the energy equation. The analysis can be carried through but the formulas are naturally more complicated and involve $S_0(r)$ and $h(r)$. Furthermore, the change in $B_z$ is immediately calculated as

$$\frac{B_z^2}{2}(r) = \frac{B_z^2}{2}(a) - \int_r^a \frac{4\pi v_r(r')}{c^2\eta_z(r')} \frac{B_\theta^2(r')}{h(r')} dr'. \quad (61)$$

Clearly the flux change is at most of order $a^2 B_\theta^2(a)/B_z(a) \propto I_p^2/B_z$. Note that Eq. (61) shows that the diamagnetism of the plasma is related very closely to the relative rates of convective particle transport (that is, $v_r$) and field transport (i.e., $c^2\eta_z \sim \chi$). Thus, $\Delta\Psi_{\rm tor}$ is of order $-(v_r a/c^2\eta_z)(I_p^2/c^2 B_z)$. This result may also be stated in the equivalent form,

$$\left|\frac{\Delta\Psi_{\rm tor}}{\Psi_{\rm tor}}\right| \simeq O\left[\frac{a^2}{q_a^2 R^2}\left(\frac{v_r a}{c^2\eta_z}\right)\right].$$

The absence of diamagnetism predicted by Eq. (61) in the absence of particle sources is specific to the assumed form of our effective resistivity tensor and may be traced to Eq. (9). In particular, it is the consequence of taking the principal axes in the toroidal–poloidal form rather than the parallel–perpendicular form of Braginskii–Spitzer theory. Conversely, if the parallel–perpendicular form for the effective resistivity had been assumed, as, for example, by Bickerton,[15] who introduced an anomalously large $\eta_\perp$ of the same order as our $\eta_\theta$, the pressure profile would be nearly flat in the absence of particle sources while $B_z$ would not have been uniform. Furthermore, Bickerton's form will not lead to the correct size for the pinch effect to account for the Coppi–Sharkey results relating to the anomalous particle flux. As we have already shown,[19] Bickerton's form cannot lead to any significant toroidal particle flux-driven currents, whereas the form suggested by us for the friction force does.

The results can also be put in a slightly different form, which relates particle fluxes to the poloidal $\beta$. Thus, we define $\beta_p$ using

$$\beta_p = \frac{8\pi\int_0^a p(r) 2\pi r\, dr}{\pi a^2 B_\theta^2(a)}. \quad (62)$$

From pressure balance and Ampère's law we obtain

$$\beta_p = 1 + \frac{B_z^2(a)}{B_\theta^2(a)} - \frac{2}{a^2 B_\theta^2(a)} \int_0^a B_z^2(r) r\, dr. \quad (63)$$

Upon making use of Eq. (55) we may rewrite this equation to obtain

$$\beta_p = 1 + \frac{8\pi}{a^2 B_\theta^2(a)} \int_0^a \frac{v_r(r) B_z^2(r) r^2\, dr}{c^2\eta_\theta}. \quad (64)$$

An equivalent and more explicit form of Eq. (64) is obtained by substituting Eq. (61) in Eq. (63). Thus we have

$$\beta_p = 1 + \frac{16\pi}{a^2 B_\theta^2(a)} \int_0^a \left(\int_r^a \frac{v_r(\rho) B_\theta^2(\rho)}{c^2\eta_z(\rho) h(\rho)} d\rho\right) r\, dr. \quad (65)$$

These results show that $\beta_p > 1$ in the presence of a particle source. Furthermore, we see that under *steady-state* conditions, $\beta_p$ as defined can be less than unity (i.e., the plasma is paramagnetic) only if there are particle sinks in the system leading to a net inward particle flux ($[\Gamma(r)/n(r)] \equiv v_r \leqslant 0$) in the system. They also show that if experimentally determined values of $v_r$ are used, $\eta_\theta$ must be very substantially large compared with toroidal resistivity to account for the experimentally observed poloidal $\beta$. This is just another manifestation of the fact that particle transport fluxes in tokamaks are anomalous. For a discussion of how Eq. (65) is modified due to thermal force terms in Ohm's law (see Sec. III F).

The assumption that $av_r/c^2\eta_z$ be small compared with unity is equivalent to the neglect in toroidal Ohm's law, of the flow-driven current $v_r B_\theta/c\eta_z$ in comparison with the Ohmic current estimated by

$$\frac{c}{4\pi}\frac{1}{r}\frac{\partial}{\partial r}(rB_\theta) \sim \frac{c}{4\pi}\frac{B_\theta}{a}.$$

Thus we have established that the particle source-free theory is more generally valid than appears at first sight. It is in fact valid as long as the particle sources are small enough for convective transport to be unimportant relative to anomalous thermal conduction. For particle sources like those due to beam heating, which are not concentrated at the edge, the analysis is less explicit. However, the earlier computational work fully covered this aspect. Clearly Eq. (58) predicts that at fixed current and $\chi$ a simultaneous increase of power and particle source leads to a net degradation of confinement due to the extra convection. It is useful to observe that an increase in power at constant $\chi$, particle source, and current must result in an increase of temperature but reduction in density (i.e., the "density clamp"[16]).

### E. Effect of noninductive current sources

Next we consider a qualitative discussion of the effects due to a noninductive source of current and power applied in addition to Ohmic heating. Following the spirit of this paper, we shall not be concerned with the details of the source, except to assume (for simplicity) that it only leads to current drive and power input, and does not introduce any new particles. The current drive source will be assumed to have a specified radial profile and magnitude. We also assume that the corresponding auxiliary heating power profile is known. Since in real experiments with current drive the total current is kept fixed and the loop volts are allowed to adjust themselves to this constraint, the theory is formulated taking this into account.

The longitudinal Ohm's law may now be written in the form

$$E_z + S_z^N = \eta_z j_z, \quad (66)$$

where $S_z^N(r)$ is the effective noninductive current source as a function of radius. Clearly we may decompose the total current density into inductive and noninductive components. Thus writing, $j_z \equiv j_z^I + j_z^N$, with $j_z^N \equiv S_z^N/\eta_z$, the inductively driven current density satisfies the usual Ohm's law

$$E_z = \eta_z j_z^I. \quad (67)$$

Clearly, a knowledge of $j_z^N$ is, in a physical sense, entirely equivalent to that of $S_z^N$, and in what follows, we shall assume for convenience that $j_z^N(r)$ is known. Associated with it is the power deposition profile $P_0(r)$. Since (by assumption) there are no particle sources, the pressure balance equation for the plasma electrons and ions that actually carry the inductive current density $j_z^I(r)$ may be written in the form

$$\frac{dp}{dr} = -\frac{j_z^I B_\theta}{c}, \tag{68}$$

where

$$\frac{c}{4\pi r}\frac{d(rB_\theta)}{dr} = j_z^I + j_z^N. \tag{69}$$

In writing these equations, we assume that the noninductive current $j_z^N$ is actually carried by a fast electron species, which contributes a negligible amount to the plasma $\beta$. Thus their main effect is to reduce the loop volts or $j_z^I$ for a given total current. It is clear from Eqs. (67) and (68) alone that, for the *same* $B_\theta(r)$, a noninductive current source leads to a lower pressure gradient.

We move on to the energy equation that takes the form

$$\frac{1}{r}\frac{d}{dr}\left(r\chi\frac{dp}{dr}\right) + E_z j_z^I + P_0(r) = 0. \tag{70}$$

Substituting from Eq. (68), we derive

$$\frac{4\pi\chi}{c^2\eta_z} = 1 - \frac{4\pi}{crB_\theta}\int_0^r j_z^N r\,dr + \frac{4\pi}{E_z crB_\theta}\int_0^r P_0(r) r\,dr$$
$$= 1 - \frac{4\pi}{crB_\theta}\int_0^r j_z^N r\,dr + \left(\frac{8\pi^2 R^2 q(r)}{cr^2 B_z V_l}\right)\int_0^r P_0(r) r\,dr, \tag{71}$$

where the loop volts $V_l$ are related to the current and $\eta_z$ by

$$V_l = \frac{R(I^{\rm tot} - I^N)}{\int_0^a (r\,dr/\eta_z)}. \tag{72}$$

It is readily seen that Eq. (71) reduces to Eq. (48) when $I^N = 0$. The physical implications of the results will now be discussed. In the absence of particle sources, at fixed total current, $I^{\rm tot}$, an increase in the noninductive current must be compensated by a decrease in loop volts and the toroidal inductively driven current density, provided $\eta_z$ remains constant. If $\eta_z$ depends only on the temperature, we can consider a situation when an increase in the noninductive current drive at nearly constant temperature is experimentally realized. In such a case, we see from Eq. (70) the loop volts will fall; Eq. (68) shows that the plasma pressure, and hence the density must decrease at constant temperature. Turning to Eq. (71), it is clear that increasing the noninductive current at constant temperature can have a complicated effect on the $\chi$ required for the energy balance to be maintained at this temperature when $P_0(r)$, $I^{\rm tot}$, and $I^N$ are given. Thus the second term on the right-hand side of Eq. (71) suggests that at constant temperature, the $\chi$ with current drive must be lower than the Ohmic value. However, the third term that relates to the extra heating input to the plasma due to the current drive source will tend to degrade the $\chi$ at constant temperature.

As an illustrative example, we consider the following scenario: Let the current density $j_z^N(r) = (I^N/P^N)P_0(r)$, where $P^N = 2\pi\int_0^a P_0(r) r\,dr$. Substituting in Eq. (71), we see that

$$\frac{4\pi\chi}{c^2\eta_z} = 1 - \left(\frac{4\pi}{crB_\theta}\right)\int_0^r P_0(r)\left(\frac{I^N}{P^N} - \frac{I^{\rm Ohmic}}{P^{\rm Ohmic}}\right) r\,dr. \tag{73}$$

In the above relation, we use the obvious definitions $I^{\rm Ohmic} \equiv I^{\rm tot} - I^N$ and $P^{\rm Ohmic} \equiv 2\pi\int_0^a E_z j_z^I r\,dr$.

For given values of $P^N$ and $I^N$, $I^{\rm Ohmic}$ and $P^{\rm Ohmic}$ are readily calculated in terms of $I^{\rm tot}$ and the assumed temperature. From the experimentalist's point of view, Eq. (73) states the conditions required at constant temperature for $\chi$ to decrease due to the simultaneous action of the current and power inputs associated with the noninductive current. Thus if $I^N/P^N > I^{\rm Ohmic}/P^{\rm Ohmic}$, the thermal diffusivity with current drive must be lower than the Ohmic value at the same temperature. On the other hand, if the current drive efficiency is low, that is, $I^N/P^N < I^{\rm Ohmic}/P^{\rm Ohmic}$, there is degradation of confinement, although somewhat reduced relative to Eq. (50) for the same values of power, current, and temperature.

Finally, we wish to stress the physical content of the results relating to pressure limitation. Only in *steady* conditions, and in the absence of particle sources is it justified to drop the $j_\theta B_z$ terms from the pressure balance relation. If this term were to be taken into account, the general scaling $n \propto I^{\rm tot}$ at constant temperature is not derivable from the pressure balance condition. Even under steady conditions, if $v_r$ and $j_\theta$ are not linked according to Eq. (53), it is not possible to relate current and density simply as indicated by the present model. Thus the direct experimental verification or otherwise of the consequences of Eq. (68) is of importance in establishing the validity of our model.

### F. Low $\beta_p$ and the role of thermal force terms in Ohm's law

In our work so far we have omitted the thermal force terms from Ohm's law. For $\beta_p \simeq 1$ this approximation should be adequate. Indeed, using our simple form of Ohm's law we were able to satisfactorily simulate a number of different discharges.[16] As will appear below, however, this procedure is inappropriate for describing low $\beta_p$ discharges.

We begin by noting the most general form of Ohm's law, given the existence of equilibrium flux (i.e., pressure) surfaces and tokamak geometry:

$$E_z\mathbf{e}_z + (\mathbf{v}\times\mathbf{B})/c = \eta\cdot\mathbf{j} - (\alpha\chi\,\nabla p\times\mathbf{B})/cp, \tag{74}$$

where $\alpha(r,t)$ is an unspecified function.

It is plain that this general form follows simply from the vectorial character of the left-hand side in the tangent plane to the flux surface spanned by the unit toroidal and poloidal vectors. The friction force may be expressed as a general linear combination of $\mathbf{j}$ and $\nabla p\times\mathbf{B}$. However, since the pressure balance relation actually relates these two vectors, it is easily seen that the tensor $\eta$ may be chosen to be diagonal without loss of generality with respect to a specified set of principal directions. In classical theory[2,3] or neoclassical the-

ory,[14] these directions are the parallel and transverse directions relative to **B**. However, our previous work shows that the anomalous particle fluxes require the toroidal and poloidal directions to be taken as the principal directions. Assuming this to be the case, we see that the term proportional to $\alpha$ in Eq. (74) extends our earlier theory. It should be emphasised that it is entirely a matter of convention whether we take the effective resistivity tensor to be diagonal and have this extra term, or alternatively, using pressure balance, eliminate this term entirely and allow a resistivity tensor with off-diagonal elements proportional to $\alpha$. With the conventions we use, namely, the effective resistivity tensor is diagonal with positive elements having the poloidal and toroidal directions as the principal directions, it will be seen that the coefficient $\alpha$ in Eq. (74) must satisfy the inequality,

$$\alpha > -\left(\frac{c^2\eta_z p}{\chi B_\theta^2}\right)\left(1+\frac{\eta_z B_z^2}{\eta_\theta B_\theta^2}\right)^{-1}$$

(for $d\ln p/d\ln n > 0$). This condition is due to the requirement [see Eq. (81)] that the total particle diffusivity must be positive. In fact, as will be seen from the following discussion, $\alpha$ is actually required by experiment to be positive.

Caution must be employed in comparing these anomalous constitutive properties in sign and magnitude with superficially similar objects in classical or neoclassical versions of Ohm's law applicable under similar circumstances. They must be first put in the same tensorial form using the pressure balance relation before a meaningful comparison can be made. Note that the thermal diffusivity $\chi$ gives the correct dimensions to the new term. Its introduction at this point embodies the important general principle first noted by Bickerton in the context of plasma physics that particle, momentum, field and energy transport rates due to turbulence are generally of the same order. This appears to be qualitatively in agreement with many tokamak transport measurements. It follows from this principle that the nondimensional constitutive function $\alpha$ is of order unity (it may, of course, be zero). The toroidal and poloidal components of Eq. (74) are as follows:

$$E_z + \frac{v_r B_\theta}{c} = \eta_z j_z - \frac{\alpha\chi}{cp}\frac{\partial p}{\partial r}B_\theta, \tag{75}$$

$$\left(-\frac{v_r B_z}{c}\right) = \eta_\theta j_\theta + \frac{\alpha\chi}{cp}\frac{\partial p}{\partial r}B_z. \tag{76}$$

Note that the thermal force is expressed in terms of $\nabla p$ rather than $\nabla T$ as is usual in classical theory. This choice is entirely consistent with our expression for the anomalous conductive heat flux. Furthermore, it can be readily shown that the results do not depend on the choice, only the conventions defining the constitutive function $\alpha$. From these equations and the pressure balance relation, it is straightforward to derive the relation

$$\beta_p = 1 + \frac{8\pi}{a^2 B_\theta^2(a)}\int_0^a \left[\frac{v_r B_z^2}{c^2\eta_\theta} - \frac{\alpha\chi B_z^2}{c^2\eta_\theta}\left(-\frac{1}{p}\frac{\partial p}{\partial r}\right)\right] r^2\,dr. \tag{77}$$

The physical implications of this result will shortly be discussed. It is clearly possible to derive, in addition, the expression

$$v_r = -\frac{1}{p}\frac{dp}{dn}\frac{\partial n}{\partial r}\left(\frac{c^2\eta_\theta p}{B_z^2}+\alpha\chi\right) - cj_z\eta_\theta\frac{B_\theta}{B_z^2}. \tag{78}$$

Substituting this expression in the toroidal Ohm's law we are led to the equation

$$E_z = \eta_z\left[j_z\left(1+\frac{\eta_\theta B_\theta^2}{\eta_z B_z^2}\right) + \frac{\partial p}{\partial r}\left(\frac{c\eta_\theta B_\theta}{\eta_z B_z^2}\right)\right]. \tag{79}$$

Finally, eliminating $j_z$ from the two preceding equations, we obtain the result

$$v_r = -\frac{1}{p}\frac{\partial p}{\partial r}\left(\frac{h(r)}{1+h(r)}\cdot\frac{c^2\eta_z p}{B_\theta^2}+\alpha\chi\right) - \frac{cE_z}{B_\theta}\frac{h(r)}{1+h(r)}. \tag{80}$$

The nondimensional function $h(r)$ was defined by Eq. (8). This equation implies the following expressions for the particle diffusivity $D$ and the inward pinch velocity $V$:

$$D = \left(\frac{1}{1+(\eta_z B_z^2/\eta_\theta B_\theta^2)}\cdot\frac{c^2\eta_z p}{B_\theta^2}+\alpha\chi\right)\frac{d\ln p}{d\ln n} \tag{81}$$

and

$$V = (cE_z/B_\theta)\{1/[1+(\eta_z B_z^2/\eta_\theta B_\theta^2)]\}. \tag{82}$$

We now discuss the implications of the preceding equations. Equation (77) indicates that in the case of a particle-source free tokamak ($v_r = 0$), the presence of the thermal force term allows the possibility of $\beta_p \leqslant 1$. As an example of this, consider the DITE steady-state shot # 30955. In this shot the current flat top ($I_p = 96\,\text{kA}$) lasts some 300 msecs, the electron energy confinement time $\tau_{Ec} \simeq 9$ msecs. The line-average electron density is also more or less constant over most of the flat-top period. The working gas is helium with no sources or sinks—just recycling at the limiter. The toroidal field $B_z = 2\,\text{T}$, $\bar{n}_e = 10^{19}\,\text{m}^{-3}$, $T_{e0} \simeq 750\,\text{eV}$, $a = 20$ cm, and $R = 80$ cm. The wave form for $\beta_p$ is essentially steady over 300 msec, at a value of $\beta_p = 0.25$. Using these values together with our prescription for $\eta_\theta$ and taking $\chi \simeq 10^4\,\text{cm}^2/\text{sec}$, then the appropriate value for $\alpha$ is estimated to be 0.13.

We note that the $\alpha$ term has no effect on the inward pinch velocity. This does depend on the ratio, $\eta_z/\eta_\theta$, however, and clearly cannot exceed $cE_z/B_\theta$. This observation shows that the $\alpha$ term by itself can never account for the inward particle pinch. It is also clear that at low $\beta_p$, the $D$ may be dominated by the thermal force term, provided it exists. Thus, an experimental measurement of $D$ and $V$ separately with sufficient accuracy can allow one to determine both $\eta_\theta$ and $\alpha\chi$. From a knowledge of these properties, the source-free steady values of $\beta_p$ can be calculated in accordance with Eq. (77) and compared directly with experiment, or conversely, from a measurement of $\beta_p(t=\infty)$, an estimate can be made of the ratio $D/\chi$ and compared with the particle transport data. It is a very clear prediction of our phenomenological model that in source-free steady conditions, the plasma $\beta_p$ cannot exceed unity and that the inward pinch velocity is bounded by a certain combination of the loop volts and the poloidal field. These predictions are independent of the size of the anomalous constitutive properties and can be directly tested by appropriate experiments.

As a somewhat different example, we consider a partic-

ular shot from JET. Like most JET discharges, this is not in steady state in the sense of our paper. By moving the plasma bodily until it touches the wall, the line-averaged density is programmed to fall "uniformly" over 10–15 sec. In other words, there is a surface sink of particles, but no volume sink. Simple estimates suggest that any neglected time derivatives in Ohm's law are unimportant, and therefore the preceding analysis should be applicable. Typical parameters are $B_{\rm tor} = 2$ T, $I_p = 3$ MA, $V_{\rm loop} = 0.6$ V, with $\beta_p \leqslant 1$. Thus assuming the plasma to be force-free ($\beta_p \simeq 0$) and setting $v_r = 0.1$ m/sec, we calculate $\alpha \simeq 0.01$.

Finally, we draw attention to a number of features arising from the above investigation. We have shown that to interpret the low $\beta_p$ experiments, the inclusion of the $\alpha$ term in Ohm's law is essential. It is straightforward to show that the parameter $\alpha$ is roughly the ratio of energy to particle confinement time. It should be noted, however, that it would not be adequate to take the electron thermal force alone on the right-hand side of Ohm's law; the anomalous poloidal resistivity is essential in obtaining the inward pinch. It is interesting to remark that the $\alpha$ term in Ohm's law plays no role in the bootstrap current. This can be clearly seen from Eq. (79). Thus, setting $E_z = 0$, we have

$$j_z = -\frac{ch(r)}{B_\theta[1+h(r)]}\frac{\partial p}{\partial r}. \tag{83}$$

Note, however, that the radial velocity $v_r$ *is* dependent on $\alpha\chi$, as shown in Eq. (80). It is clear from our analysis that the presence of a particle source is the most essential feature in establishing $\beta_p > 1$ in a macroscopically steady state, namely the regime of reactor interest. This conclusion is independent of whether or not there are anomalous thermal force type terms. It is also clear that the actual achievable values will be limited by transport processes.

### G. Basis of $\eta_z$-$\eta_\theta$ representation

We now discuss our particular choice of resistivity tensor $\eta_\theta$, $\eta_z$. We have found that this is the simplest form that leads to results in agreement with experiment. It should be pointed out that turbulent constitutive properties need not respect the symmetries of classical or neoclassical theories in all respects. We do not know of any proof that in the presence of electromagnetic turbulence measured in present-day tokamaks with $k_\perp \rho_i \simeq 0.1$ the directions parallel and perpendicular to the *mean* magnetic field have any particular significance as opposed to the toroidal and poloidal directions. Indeed, a strong argument may be made that turbulent electrostatic fluctuations break the *local* gyroangle symmetry seen by individual charged particles but may respect the global azimuthal symmetry and the equivalence with respect to that symmetry of any poloidal plane. Such "spontaneous symmetry breaking" of a local symmetry is commonplace in physics. The excursions of a particle due to turbulent $\mathbf{E}\times\mathbf{B}$ are far larger than Larmor radii, even for ions.

It is widely accepted that the electrostatic turbulence thought to be responsible for particle and ion anomalous transport obeys the wave number ordering $k_\theta$, $k_r \gg k_\parallel$. It follows readily that $k_{\rm pol}(B_{\rm pol}/B_{\rm tor}) \simeq k_{\rm tor}$. Since the turbulent "friction forces" $f$ in Ohm's law on a mean magnetic surface are proportional to the square of the fluctuating electric field, it is plain that we must at least roughly have $f_\theta^{\rm turb} \simeq f_z^{\rm turb}(B_z/B_\theta)^2$, as suggested in our model of the effective resistivity tensor.

## IV. THE TIME-DEPENDENT CASE

### A. General considerations

The theory discussed in the preceding section can be viewed in two ways. First, it represents an exploration of the properties of the steady-state transport equations given the sources and the assumed constitutive relations. In this view, there is no suggestion that the results necessarily describe a real experiment. Second, we might consider experiments for which certain time-scale assumptions are empirically found to be valid. Thus, macroscopic states of tokamaks in which the external sources are held steady for time scales very much larger than the energy confinement time and the resistive diffusion time, could be described by our theory in the absence of macroscopic modes such as the sawtooth. As far as we are aware, discharges that are sawtooth-free, either due to external stabilization or some internal mechanism, provide examples of this type.

Next we turn to a different interpretation of the preceding results and indicate a generalization of them to discharges that have sawtooth oscillations, but are otherwise in a macroscopically stationary state. We shall demonstrate that the sawtooth time-averaged equations have the same mathematical structure as the steady equations considered previously, provided certain experimental facts are properly taken into account. It is important to note that we do not mean to imply that the constitutive properties that pertain to sawtoothing discharges necessarily have the same functional dependence or numerical values to those obtained for nonsawtoothing discharges. However, the formal similarity of the equations does mean that many of the results obtained for truly steady discharges can be taken over *mutatis mutandis* to the sawtoothing case.

To make the ideas definite, we consider the following situation. We assume that the total current in the plasma is kept fixed, as well as the toroidal field. We also assume for simplicity that the particle and energy sources are kept fixed. Let us consider discharges that are macroscopically stationary, in the sense that sawtoothing is periodic with a period $\tau_s$. To avoid discussing monsters in the present context, we assume, with Goedheer and Westerhof that $\tau_{\rm flattop} \gg \tau_{\rm resistive} \geqslant \tau_s$. Experimental evidence[1-4] suggests that the plasma properties, such as density, temperature, and $q$ can be written as follows:

$$T_e(r,\theta,z,t) \equiv T_0(r) + T_1(r,t) + \tilde{T}(r,\theta,z,t). \tag{84}$$

Clearly, $T_0(r)$ is the mean temperature at a particular radius, the average being taken over many sawtooth periods and over the flux surfaces (concentric circular by assumption). Here $T_1(r,t)$ is the periodic temperature variation at that radius due to the sawtooth activity with an $m = 0$ symmetry. In addition, $\tilde{T}(r,\theta,z,t)$ represents the higher $m$ periodic perturbations due to nonlinear coupling. In toroidal geometry, $r$ would have to be replaced by an effective flux-surface coordinate. A decomposition of this nature can be applied to all

the macroscopic plasma variables and constitutive properties considered in the previous section. Many experimental techniques already imply such a decomposition procedure. Thus in TEXT,[6] $T_0(r)$ and $q(r)$ are measured by ensemble-averaging procedures (involving many shots). However, in other experiments, JET, for example,[1,2] $q$ is measured at a point instantaneously throughout a sawtoothing discharge. The fact that the variations of this measured property are small and periodic, lends credence to the suggestion that the time-averaged quantity obtained over many sawtooth periods is essentially constant and depends on the external sources. It also indicates that the periodic perturbation of $q$, in particular, are not significantly larger than experimental error, and certainly $q(0)$ does not appear to oscillate between 0.7 and 1.0, for example, in a sawtooth cycle. In the case of density and temperature, much more complete data are available regarding the periodic perturbations. Excluding the so-called giant sawteeth, $T_1(r,t)$ and $n_1(r,t)$ are typically 10%–20% of the mean values.[13] This perturbation occurs mostly within the $q=1$ surface, although the sawtooth pulse propagates to the edge of the plasma following a crash.

We wish to stress once more that quantities like $T_0(r)$ and $\chi_0$ appearing in expansions such as Eq. (84) must not be thought of as values that would be expected in the absence of sawtoothing. They are actually time averages evaluated over a complete sawtooth period and can certainly depend upon the amplitude of the sawtooth, for example.

Next we proceed to discuss the time-periodic behavior of $\chi$. It must be stated that there is very little direct evidence from experiment of sufficient precision or generality to make definite statements about $\chi$. Our discussion will be based on a set of hypotheses that appear to have some experimental support. At this point in time we are not aware of any other work, numerical or analytic, in which the time-periodic behavior of $\chi$ appropriate to sawtoothing tokamaks is discussed in any detail. We assume first that $\chi(r,\theta,z,t)$ may be decomposed, as in Eq. (84). We further assume that the time-averaged part $\chi_0(r)$ is essentially given by a monotonic increasing function of $r$, as suggested by certain transport analyses of data. We specifically wish to avoid a uniform $\chi$ with a large constant value within the $q\leqslant 1$ region. The behavior of $\chi_1$ is crucial to any sawtooth model. The complete reconnection model requires that $\chi_1(r,t)$ take on a very large value relative to $\chi_0$ every time a crash occurs, everywhere within the $q\leqslant 1$ zone. As discussed by Goedheer and Westerhof, actual sawtooth oscillations do not appear to support such a model. Indeed, it appears that experiment is better described by requiring $\chi_1(r,t)$ to be localized near the $q=1$ radius, and also localized in time so that $\chi_1$ is significant only during the crash phase. It is clear from the structure of the energy equation that if $\chi_1$ were to have these properties, the only effect of the crash on the pressure profile would be to flatten it near the $q=1$ radius, just after the crash. There is at present no theory available that is able to predict either $\chi_0(r)$ or $\chi_1(r,t)$ from first principles and account for the observed transport data. The same statement is true for $\eta_\theta$, even if $\eta_z$ could be assumed to be given by Spitzer or neoclassical theory in a time-dependent situation. As we have seen, during the slow ramp phase, in the absence of particle sources within the confinement and sawtooth zones, it may be possible to neglect convective flows and inertia. These assumptions will fail to hold during the crash phase, and certainly the full radial momentum equation with inertial terms and the poloidal Ohm's law with anomalous resistivity are needed to give a complete dynamical account of the periodic sawtooth phenomenon. However, by virtue of our assumptions about $\chi$, we can show that by *assuming* a periodic solution to exist, the time averages (over a complete sawtooth period and the mean flux surfaces) such as $T_0(r)$ do indeed obey the steady-state equations developed in the previous sections. This is shown explicitly for the energy equation. The identical arguments apply to all the other governing equations. Thus consider the energy equation (we neglect the self-interactions of the $m>0$ components),

$$\frac{3}{2}\left(\frac{\partial p}{\partial t}+\frac{1}{r}\frac{\partial(rv_r p)}{\partial r}\right)+\frac{p}{r}\frac{\partial(rv_r)}{\partial r}$$
$$=\frac{1}{r}\frac{\partial[r\chi(\partial p/\partial r)]}{\partial r}+E_z j_z+P(r,t). \tag{85}$$

Every dependent variable may be expressed as a Fourier series, such as

$$p(r,t)\equiv p_0(r)+\sum_{n=1}^{\infty}p_n(r)\cos\left(\frac{2\pi nt}{\tau_s}+\delta_n\right). \tag{86}$$

Substituting expressions like those given by Eq. (86) in Eq. (85) and averaging over a period $\tau_s$, we obtain the equation

$$\frac{3}{2}\frac{\partial}{r\,\partial r}\{r[v_{r0}(r)p_0(r)+\langle v_{r1}(r,t)p_1(r,t)\rangle]\}$$
$$=-\frac{p_0(r)}{r}\frac{\partial[rv_{r0}(r)]}{\partial r}-\left\langle\frac{p_1(r,t)}{r}\frac{\partial[rv_{r1}(r,t)]}{\partial r}\right\rangle$$
$$+\frac{\partial[r\chi_0(\partial p_0/\partial r)]}{r\partial r}+E_{z0}j_{z0}+P_0(r)$$
$$+\frac{\partial[r\langle\chi_1(\partial p_1/\partial r)\rangle]}{r\,\partial r}+\langle E_{z1}j_{z1}\rangle. \tag{87}$$

From our previous assumptions and the averaged continuity equation, $v_{r0}$ is negligible if there are no steady particle sources. Clearly the second-order averages appearing in Eq. (87) represent net losses due to sawtooth pulsations. Bearing in mind that the definition of $\chi_0$ is related to the *time-averaged heat flux* including all forms of heat loss apart from radiation and the explicit convective loss term, it is clear that the losses represented by these second-order averages are already operationally, taken into account by the $\chi_0(\partial p_0/\partial r)$ term. To avoid double counting, we make use of this property of $\chi_0$ and consistently drop all explicit second-order averages in Eq. (87). In doing this, we recognize explicitly that the $\chi_0$ that appears in Eq. (87) need not necessarily be the anomalous thermal diffusivity of the plasma pertaining to sawtooth-free conditions. It is, however, the quantity obtained by a transport analysis of sawtoothing discharges.

The same arguments applied to the other conservation equations result in the transport equations discussed previously to sufficient accuracy, provided we assume from experiment that a periodic state exists with period small compared to the pulse length over which the external sources are held constant. We note, however, that the periodicity is *as-*

*sumed* from experiment, and not deduced from the full time-dependent equations. Therefore, the precise relationship between ramp/period time scale $\tau_s$, the resistive time scale, and the energy confinement time scale $a^2/\chi_0$ cannot be derived without solving the nonlinear equations governing $T_1$, etc. Indeed, the solution must also, in principle, involve the higher $m$ perturbations and the inertia terms to describe the rapid crash. In the light of this discussion, the results of the previous sections can clearly be applied to sawtoothing discharges, with suitable interpretation.

### B. An approach to periodic sawtooth behavior

Next we consider some general ideas relating to a dynamical description of periodic sawtooth behavior in tokamaks under stationary external conditions. As discussed in the previous section, a complete theory is only possible if the full set of nonlinear equations governing dynamical variables like $T_1(r,t)$ and $\tilde{T}(r,\theta,z,t)$ are known. In view of the fact that at the very least, energy transport in tokamaks is anomalous, these equations cannot simply be taken to be the two-fluid Braginskii equations. They must involve the anomalous thermal diffusivity, viscosity, and possibly an anomalous resistivity tensor. Experimentally, these turbulent constitutive properties are not known in time-dependent situations, such as those arising in sawteeth or in the presence of gross modes like the $m = 1$ or $m = 2$. Thus, inevitably, all present theoretical approaches to the problem involve a number of more or less arbitrary assumptions. As an example, we may cite the work of Aydemir *et al.*,[12] where periodic reconnecting sawteeth are obtained from a set of fluid equations under specific assumptions relating to $\chi$ and $\eta$. Unfortunately, the nonuniqueness of such models was also shown by these authors who obtained nonperiodic (i.e., chaotic) time-dependent behavior making equally plausible but physically different assumptions about $\chi$. Furthermore, Goedheer and Westerhof show that many features of experiment relating to sawtoothing discharges cannot be satisfactorily accounted by reconnection models. They also showed that by adopting certain ideas of Dubois and Samain, relating to the $m = 1$ mode, a semiempirical description can be given of the whole sawtooth. In view of these difficulties we do not attempt a complete deductive theory of periodic sawteeth but construct a very simple zero-dimensional description of the turbulent sawtooth model of Goedheer and Westerhof.

We begin by listing the essential features of the Goedheer–Westerhof model. The sawtooth ramp is described in terms of number density, temperature, and $q$, which are taken to be functions of $r$ and $t$. These dependent variables satisfy a set of transport equations with assumed sources and a $\chi$ profile. During the ramp the temperature and the density evolve in such a way that the central values increase linearly with time, as indeed suggested by experiment. Since $q(0)$ is taken to be below unity at the start of the ramp phase, Goedheer and Westerhof suppose that there is an $m = 1$ island with certain properties, superposed on the underlying equilibrium. Taking the observed sawtooth period as given, Goedheer and Westerhof determine certain constants that relate to the Dubois–Samain threshold for a rapid crash to occur. At the appropriate amplitude they simulate the crash by means of a large increase in the local value of $\chi$, the effect of which is to leave the $q$ profile relatively unaltered, but bring down the central temperature abruptly to its initial value at the start of the ramp phase. The main effect on the profiles is a distinct flattening near the $q = 1$ radius, which is itself not significantly changed. There are thus three essential physical parameters in this simulation; $\tau_s$, the time scale of the ramp and the sawtooth repetition period is taken from experiment and is (usually) small compared with the resistive diffusion time scale; the sawtooth amplitude $\Delta T/T_0$, where $\Delta T$ is the change in central temperature before and after the crash, and $T_0$ is the average temperature. Finally, it is the increase in $\chi$ attributed to the turbulence during the crash, which actually sets the time scale of the crash itself. This last time scale is known from experiment to be of order 100 $\mu$sec, and is therefore small compared with $\tau_s$.

We next consider a system of model equations that mathematically represent the above ideas. We do not claim to have derived the equations from some more complete set of plasma equations such as those considered in the preceding sections. They are, however, motivated by the temporal structure present in sawtoothing discharges and the forms of the plasma equations. It is useful in the following discussion to bear in mind that periodic behavior of dynamic systems suggests that, at most, two dynamical variables and an autonomous nonlinear set of equations coupling the time evolution of these variables are involved. For the purposes of discussion, we consider the central temperature perturbation $T(0,t)$ suitably normalized and some nondimensional turbulence amplitude (it could be the magnitude of the magnetic field fluctuation, for example) as our basic dynamical variables $Y(t)$ and $X(t)$, respectively. As we are at the moment interested only in the dynamical description of the time evolution, the spatial variations described by the full plasma equations are not covered by our simplified model. The reasons for choosing this particular physical interpretation for the dynamical variables will become clearer as the properties of the equations and the solutions are derived.

Let $Y(t)$ and $X(t)$ be governed by the following nonlinear ordinary differential equations:

$$\frac{dY}{dt} = \frac{1}{\tau_s} - \frac{\lambda X}{\tau_s}, \tag{88}$$

$$\frac{1}{2}\frac{dX}{dt} = \frac{\lambda}{\tau_s}(Y - 1)X. \tag{89}$$

In the preceding equations, $\tau_s$ is a time scale characteristic of the equilibrium properties of the discharge, while $\lambda$ is a nondimensional constant that we assume to be large compared with unity. A possible physical interpretation of $\lambda$, $\tau_s$ will shortly be made apparent. We also note here that in spite of the fact that the equations look rather special and involve a single nondimensional parameter $\lambda$ (by nondimensionalizing time using $t/\tau_s$, we can clearly remove $\tau_s$), many other, apparently more general equations can be reduced to this form by elementary transformations. In this sense, the equations stated appear to represent a canonical form for a class of equations with very similar dynamical behavior (namely, lead to sawtoothlike periodic time series).

We note that the system has a unique steady solution, $Y \equiv 1, X \equiv 1/\lambda$. It is easy to verify that this solution is a stable center in the phase plane. The second important property of the above system is that if $X$ is non-negative at $t = 0$, it must remain so for all times. Furthermore, it is easily shown that the Eqs. (88) and (89) possess the exact constant of the motion, $I(t)$, where

$$I(t) \equiv (Y-1)^2 - (1/\lambda)\log X + X. \tag{90}$$

Thus, we must have $dI/dt = 0$ for all $t$. This fact and the assumed largeness of $\lambda$ can be used to integrate Eqs. (88) and (89) in terms of nonelementary integrals and also obtain a complete qualitative description of the motion for initial conditions, such that $Y(0) = 0$ and $X(0) =$ any small positive number. Although an analytic treatment is possible, it turns out to be simpler to proceed numerically, and we show an example of such a numerical integration of the equations in Figs. 1–4. Thus taking the time step $\Delta t$ to be $10^{-6}$ sec, $\tau_s$ to be 5 msec, $\lambda = 10$, and normalizing the amplitude such that $Y_{\max} = 2$, we find that the quantity $10 + Y(t)$ shows the characteristic sawtooth waveform, periodically repeating itself, with a period of order 12 msec (see Fig. 1). The variable $X(t)$ is seen to be very small during the ramp phase (see Fig. 2). Its "spikey" character during the crash phase is typical of Eq. (89). The parameter $\lambda$ is related to the ratio of the crash time scale to the period of oscillation as follows:

$$\tau_{\text{crash}}/\tau_{\text{period}} = \log\lambda/\lambda. \tag{91}$$

The quantity $\tau_s$ is seen to be typically of the order of the period (and of course to that of the ramp phase $\tau_{\text{ramp}}$) and is in fact related to the latter (when $Y_{\max}$ is normalized to 2) through the equation

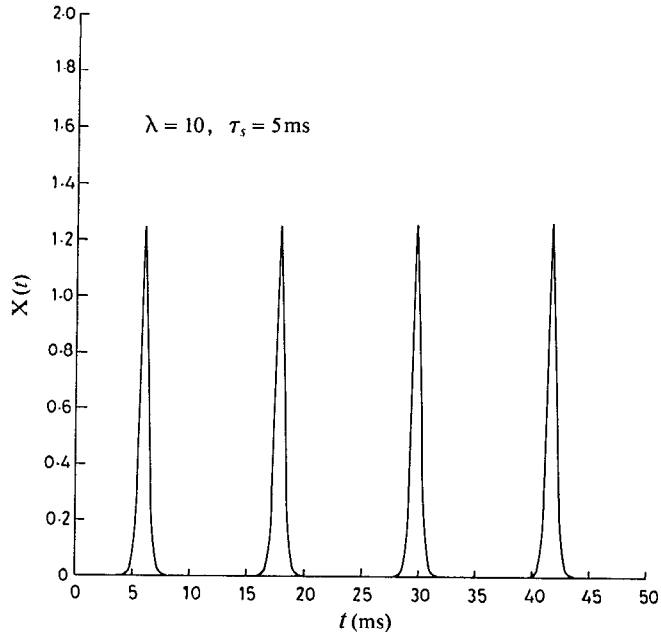


FIG. 2. Calculated $X(t)$ waveform corresponding to Fig. 1. The initial condition is $X(0) = (1/\lambda)\exp(-\lambda)$.

$$\tau_{\text{period}} = 2\tau_s[1 + (\log\lambda/\lambda)]. \tag{92}$$

For the value of $\lambda$ chosen, the calculated period ($\approx 12$ msec) is in good agreement with that predicted by the approximate formula, Eq. (92). The crash time, $\tau_{\text{crash}} \approx 2.8$ msec, is also in agreement with Eq. (91). These results have been subjected to a further numerical check in Figs. 3 and 4, which pres-

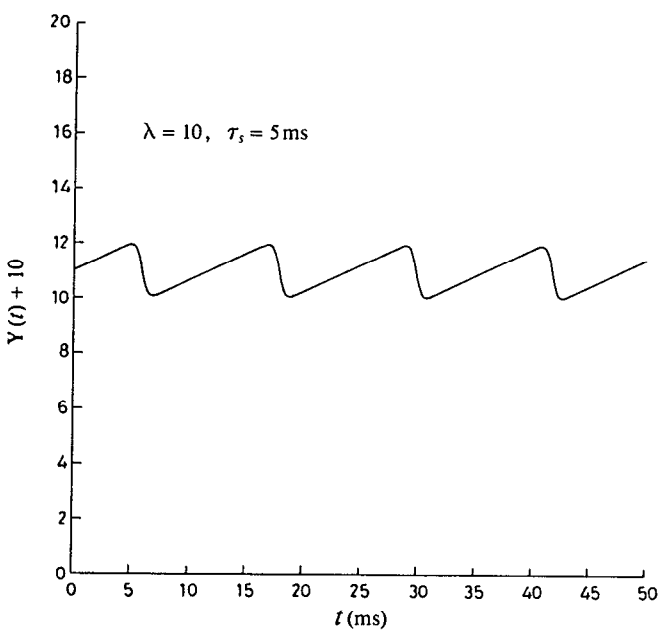


FIG. 1. Calculated sawtooth waveform of $Y(t) + 10$ for $\Delta t = 1$ μsec, $\lambda = 10$, $\tau_s = 5$ msec case. Note that $Y_{\max} = 2$.

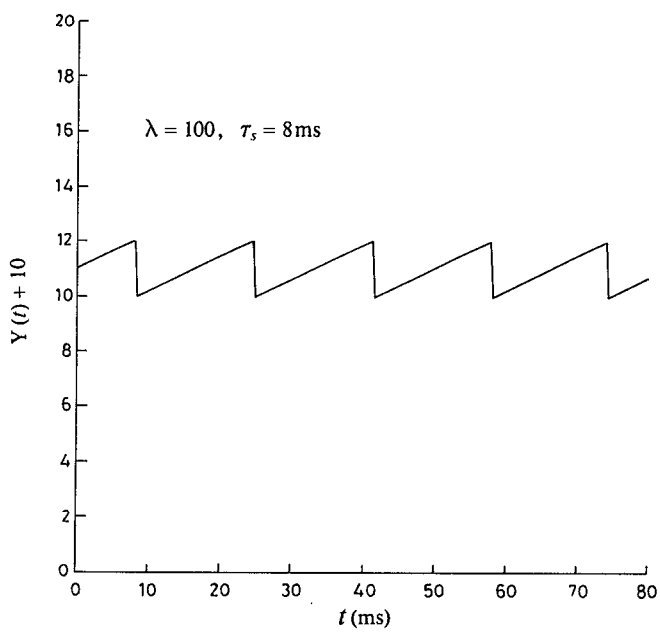


FIG. 3. Calculated sawtooth waveform of $Y(t) + 10$ for $\Delta t = 0.1$ μsec, $\lambda = 100$, $\tau_s = 8$ msec case. Note that $Y_{\max} = 2$. Note the much sharper "sawteeth."

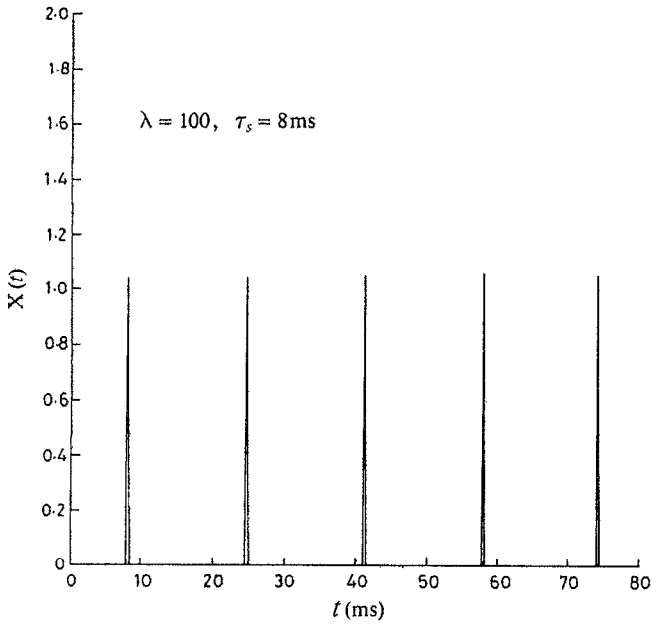


FIG. 4. Calculated $X(t)$ waveform corresponding to Fig. 3. The initial condition is $X(0) = (1/\lambda)\exp(-\lambda)$.

ent the calculated waveforms of the variables for a different set of parameters: $\Delta t = 10^{-7}$ sec, $\tau_s = 8$ msec, $\lambda = 100$. The estimated values of $\tau_{\text{period}} \approx 17$ msec, $\tau_{\text{crash}} \approx 800\ \mu$sec, and $X_{\max} \approx 1.05$ are clearly in agreement with the values obtained by the direct numerical simulations shown. In particular, the scaling of the crash time scale and the turbulence amplitude with $\lambda$ is made evident. It is of interest to note that the inevitable truncation and roundoff errors in the numerical solution have not affected the results (as compared with analytic theory) to any measurable extent. This indicates a certain robustness of the governing differential equations to small perturbations. It should be stressed that this system of equations is the simplest mathematical representation (in terms of autonomous differential equations) of any sawtoothing time series characterized as in Fig. 1. Thus any model of time evolution in tokamaks that purports to describe a time series of this type in gross terms should be reducible mathematically to the system considered or one similar to it. Such a deductive derivation would of course automatically result in scaling relations for $\lambda$, $\tau_s$, and the amplitude levels in terms of basic tokamak parameters such as $q_a$ and $\chi$.

The structure of Eqs. (88) and (89) for large $\lambda$ shows that $Y(t)$ linearly increases with time from 0 to 2. When it is less than unity, $X$ is essentially damped, which does not, however, mean that it is zero in reality. Since we propose to interpret $X$ as a measure of the turbulence level near the $q = 1$ radius, during the ramp phase $X$ can be expected to be at the noise level. As $Y$ continue to increase past unity, $\log X$ increases with time from a large negative value. When $X$ is of order $1/\lambda$, $Y$ must abruptly fall to its initial value of zero as $X$ grows and decays during the "crash." The variable $Y$ is therefore conveniently interpreted as a nondimensional, normalized measure of the temperature perturbation at $r = 0$ relative to its mean value. The maximum value of $X$ expected is $O(1)$, indicating that the crash is indeed associated with finite amplitude turbulence.

While the problem of identifying the parameters $\lambda$ and $\tau_s$ from the full set of transport equations with prescribed $\chi$, $\eta_z$, $\eta_\theta$ appropriate to experiment remains open, we put forward arguments that make use of earlier results in connection with the steady solution. Thus assuming $Y = 1$ and $X = 1/\lambda$, and interpreting $X$ as the square of the $m = 1$ saturated neighboring equilibrium derived in our previous paper,[21] we would estimate that $\lambda \simeq [d \log \eta_z(r_i)/d \log q(r_i)]^2$, where $q(r_i) = 1$. Making use of the relations derived in previous sections, we set $\eta_z \sim \chi(r_i)$. Thus, in the case of sawtooth-free discharges at least, the value of $\lambda$ is seen to be related in this interpretation to the behavior of $\chi$ and $q$ at resonance, provided $q_0 \leqslant 1$. These considerations lead to the estimates discussed in Sec. II. Finally, in the specific case of the monster, $\tau_s$ is experimentally known to be of the order of the resistive diffusion time, if not larger.

## V. CONCLUSIONS

The principal results of the paper have been reviewed in Sec. II and derived in detail in Sec. III. Several different cases of physical interest have been discussed in a unified framework, highlighting the scaling relationships implied jointly by the conservation laws and the assumed constitutive properties. All these relations are, in principle, experimentally testable and can therefore be expected to throw more light on the nature and origin of anomalous transport in tokamaks. It is important to note that relationships derived are actually consequences of the *forms* of the constitutive relations and the sources, not the details of the mechanisms that might be responsible for their numerical values or scaling behavior with plasma properties. This structural generality enables them to be used in conjunction with experimental data in several different situations to study tokamak transport. Arguments are advanced to show that the results may be applied to both sawtooth-free and sawtoothing discharges with a suitable interpretation of variables. A simple analytical model is presented and used to represent certain gross features of sawtoothing behavior. The results of this paper are intended to be complementary to detailed numerical simulations and to provide physical insight to help understand the results of such simulations and the large body of experimental data relating to transport in tokamaks.

## ACKNOWLEDGMENTS

We are grateful to our colleagues, Jack Connor, Jim Hastie, Jan Hugill, and David Ward for stimulating criticisms and helpful suggestions. Thanks are due to Brian Keen for permission to publish JET data.

[1] J. O'Rourke, J. Blum, J. G. Cordey, A. Edwards, N. Gottardi, B. Keegan, E. Lazzaro, G. Magyar, Y. Stephan, P. Stubberfield, D. Verón, and D. Zasche, in *Proceedings of the 15th European Conference on Controlled Fusion and Plasma Heating*, Dubrovnik (European Physical Society, Geneva, 1988), Vol. 12B, Part I, p. 155.

[2] J. O'Rourke and E. Lazzaro, in *Proceedings of the 17th European Conference on Controlled Fusion and Plasma Heating*, Amsterdam (European

Physical Society, Geneva, 1990), Vol. 14B, Part I, p. 343.
[3] D. J. Campbell, L. Baylor, V. P. Bhatnagar, M. Bures, A. Cheetham, J. G. Cordey, G. A. Cottrell, J. de Haas, A. W. Edwards, L. G. Eriksson, A. Gondhalekar, N. Gottardi, R. J. Hastie, T. Hellsten, J. Jacquinot, E. Lazzaro, L. McCarthy, P. D. Morgan, J. O'Rourke, D. Pearson, F. Pegoraro, F. Porcelli, G. L. Schmidt, J. A. Snipes, D. F. H. Start, P. Stubberfield, P. R. Thomas, K. Thomsen, B. J. D. Tubbing, and J. A. Wesson, in *Plasma Physics and Controlled Fusion Research* (International Atomic Energy Agency, Vienna, 1989), Vol. I, p. 377.
[4] R. D. Gill, A. W. Edwards, B. Keegan, E. Lazzaro, J. O'Rourke, A. Weller, and D. Zasche, in *Proceedings of the 16th European Conference on Controlled Fusion and Plasma Heating,* Venice (European Physical Society, Geneva, 1989), Vol. 13B, Part II, p. 469; F. M. Levinton, R. J. Fonck, G. M. Gammel, R. Kaita, H. W. Kugel, E. T. Powell, and D. W. Roberts, Phys. Rev. Lett. **61**, 2060 (1989).
[5] TEXTOR Team, in *Plasma Physics and Controlled Fusion Research* (International Atomic Energy Agency, Vienna, 1989), Vol. I, p. 331.
[6] A. J. Wootton, M. Austin, R. D. Bengtson, J. A. Boedo, R. V. Bravenec, D. L. Brower, J. Chen, G. Cima, K. A. Conner, T. P. Crowley, P. H. Diamond, R. Durst, P. H. Edmonds, S. P. Fan, J. C. Forster, M. S. Foster, R. F. Gandy, K. W. Gentle, G. A. Hallock, R. L. Hickock, L. K. Huang, W. C. Jennings, J. Y. Kim, S. Kim, H. Lin, N. C. Luhmann, Jr., S. C. McCool, W. H. Miner, A. Ouroua, D. M. Patterson, W. A. Peebles, P. E. Phillips, T. L. Rhodes, B. Richards, C. P. Ritz, D. W. Ross, W. L. Rowan, P. M. Schoch, D. Sing, E. Synakowski, P. W. Terry, D. Thomas, K. Wenzel, W. P. West, J. C. Wiley, D. Wroblewski, X. Z. Yang, X. H. Yu, and Z. Zhang, in *Plasma Physics and Controlled Fusion Research* (International Atomic Energy Agency, Vienna, 1989), Vol. I, p. 293.
[7] P. Descamps, G. Van Wassenhove, R. Koch, A. M. Messiaen, P. E. Vandenplas, J. B. Lister, and Ph. Marmillod, Phys. Lett. A **143**, 311 (1990).
[8] R. E. Denton, J. F. Drake, R. G. Kleva, and D. A. Boyd, Phys. Rev. Lett. **56**, 2477 (1986).
[9] A. Bondeson, Nucl. Fusion **26**, 929 (1986).
[10] P. Kirby, Comput. Phys. Commun. **47**, 17 (1987).
[11] J. A. Holmes, B. A. Carreras, and L. A. Charlton, Phys. Fluids B **1**, 788 (1989).
[12] A. Y. Aydemir, J. C. Wiley, and D. W. Ross, Phys. Fluids B **1**, 774 (1989).
[13] W. J. Goedheer and E. Westerhof, Nucl. Fusion **28**, 565 (1988).
[14] J. S. Kim and J. M. Greene, Plasma Phys. Controlled Fusion **31**, 1069 (1989).
[15] R. J. Bickerton, J. Phys. D **11**, 1781 (1978).
[16] F. A. Haas and A. Thyagaraja, Plasma Phys. Controlled Fusion **28**, 1093 (1986).
[17] M. A. Dubois and A. Samain, Nucl. Fusion **20**, 1101 (1980).
[18] B. Coppi and N. Sharkey, Nucl. Fusion **21**, 1363 (1981).
[19] A. Thyagaraja and F. A. Haas, Europhys. Lett. **5**, 425 (1988).
[20] F. A. Haas and A. Thyagaraja, Phys. Scr. **40**, 484 (1989).
[21] A. Thyagaraja and F. A. Haas, Phys. Fluids B **3**, 580 (1991).
[22] S. Hamaguchi and W. Horton, Phys. Fluids B **2**, 1833 (1990).
[23] E. M. Lifshitz and L. P. Pitaevskii, *Physical Kinetics* (Pergamon, Oxford, 1981), p. 244.